NASA CR-2654

NASA CONTRACTOR REPORT

NASA CR-26

REDUCTION OF WIND-TUNNEL WALL INTERFERENCE BY CONTROLLED WALL FLOW

Samuel Bernstein and Robert G. Joppa

Prepared by
UNIVERSITY OF WASHINGTON Wash. Univ., Seattle.
Seattle, Wash. 98195
for Langley Research Center

NATIONAL AERONAUTICS AND SPACE ADMINISTRATION · WASHINGTON, D. C. · MARCH 1976

1. Report No. NASA CR-2654	2. Government Accession No.	3. Recipient's Catalog No.
4. Title and Subtitle REDUCTION OF WIND-TUNNEL WALL INTERFERENCE by CONTROLLED WALL FLOW		5. Report Date March 1976
		6. Performing Organization Code
7. Author(s) Samuel Bernstein and Robert G. Joppa		8. Performing Organization Report No.
		10. Work Unit No.
9. Performing Organization Name and Address Department of Aeronautics and Astronautics University of Washington Seattle, Washington 98195		
		11. Contract or Grant No. NGL-48-002-010
		13. Type of Report and Period Covered Contractor Report
12. Sponsoring Agency Name and Address National Aeronautics and Space Administration Washington, DC 20546		
		14. Sponsoring Agency Code

15. Supplementary Notes
Langley technical monitor: Harry H. Heyson

Topical Report

16. Abstract

Corrections for wind tunnel wall interference are applied successfully to high lift models when the model to tunnel size ratio is small. The accuracy of the corrections becomes poorer when larger models are tested. An alternate method of testing was developed during this study, in which flow through the porous walls of the tunnel was actively controlled so as to approximate free air conditions in the neighborhood of the model during the test. The amount and distribution of the controlled flow through the walls is computed using a potential flow representation of the model based on the measured lift.

Theoretical analysis is presented to prove the convergence of the method to free air conditions and to substantiate the general three-dimensional theory of operation when the normal flow distribution is continuous. In practice the flow through the walls is through a pattern of holes so that if the mass flow through a section of wall is matched to the theoretical value, the momentum will be mismatched, and vice versa. An analysis was made of expected error due to such flow mismatch, and it is shown that the error decreases rapidly with increased porosity ratio.

A two-dimensional tunnel was constructed to evaluate the concept. Results show that substantial reduction of wall interference may be achieved with relatively low values of porosity of actively controlled walls.

17. Key Words (Suggested by Author(s)) Wind-Tunnels Wall Interference	18. Distribution Statement Unclassified - Unlimited Subject Category 09

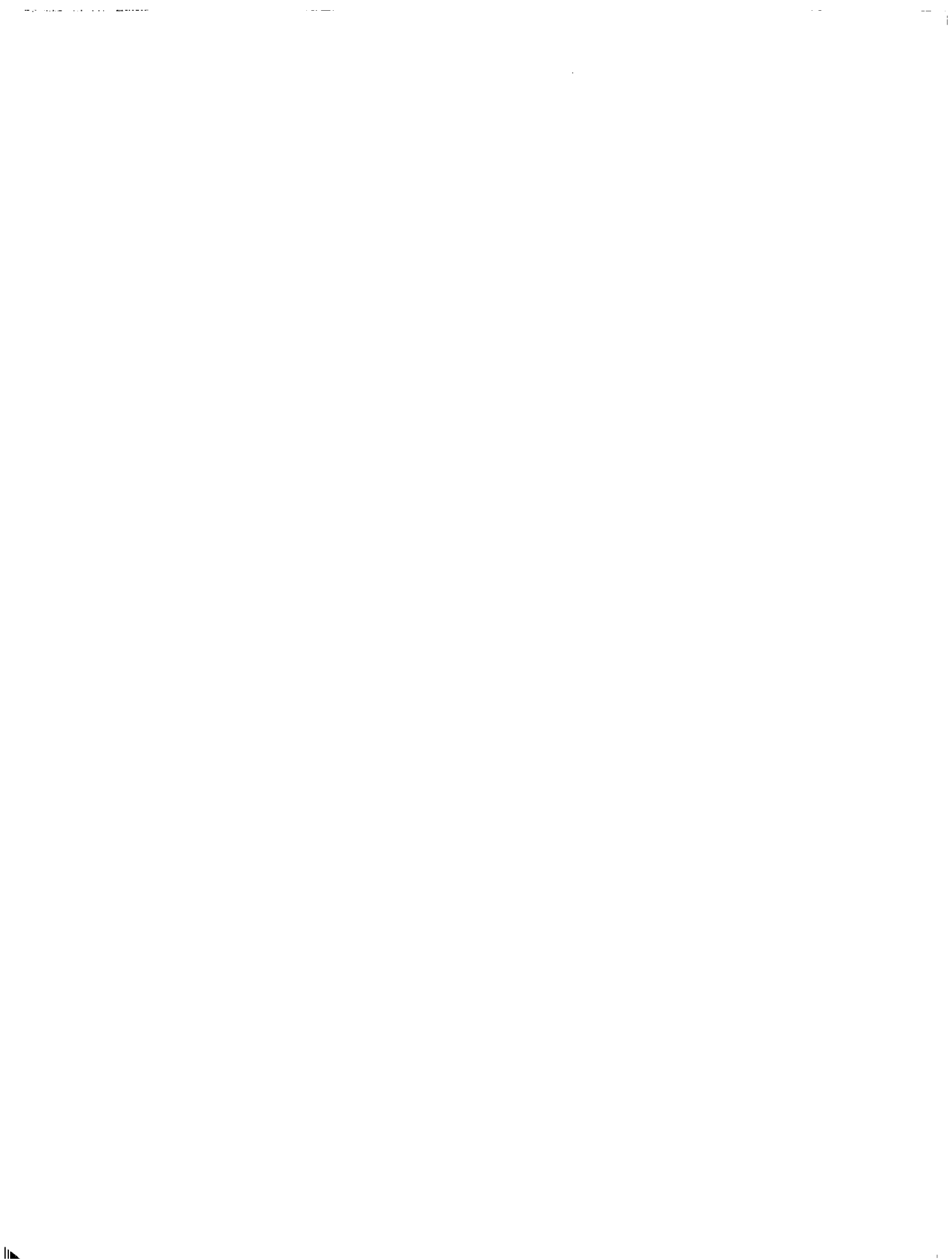| 19. Security Classif. (of this report) Unclassified	20. Security Classif. (of this page) Unclassified	21. No. of Pages 57	22. Price* $4.25

TABLE OF CONTENTS

LIST OF FIGURES

REDUCTION OF WIND TUNNEL WALL

INTERFERENCE BY CONTROLLED WALL FLOW

SUMMARY

Corrections for wind tunnel wall interference are applied
successfully to high lift models when the model to tunnel size
ratio is small. The accuracy of the corrections becomes poorer
when larger models are tested. An alternate method of testing
was developed during this study, in which flow through the
porous walls of the tunnel was actively controlled so as to
approximate free air conditions in the neighborhood of the model
during the test. The amount and distribution of the controlled
flow through the walls is computed using a potential flow repre-
sentation of the model based on the measured lift.

Theoretical analysis is presented to prove the convergence
of the method to free air conditions and to substantiate the
general three-dimensional theory of operation when the normal
flow distribution is continuous. In practice the flow through
the walls is through a pattern of holes so that if the mass flow
through a section of wall is matched to the theoretical value,
the momentum will be mismatched, and vice versa. An analysis
was made of expected error due to such flow mismatch, and it is
shown that the error decreases rapidly with increased porosity
ratio.

A two-dimensional tunnel was constructed to evaluate the
concept. Results show that substantial reduction of wall inter-
ference may be achieved with relatively low values of porosity
of actively controlled walls.

INTRODUCTION

Interest in wind tunnel interference has increased in recent years with increasing interest in V/STOL vehicles. The requirement to simulate flight vehicles at extreme lift coefficients, with possible partial flow separation at hovering flight or transition flight, has presented new challenges for wind tunnel designers. The problem is amplified by the necessity to test models with large physical dimensions while at the same time preserving a favorable vehicle to wind tunnel size ratio.

The need to test large models in V/STOL vehicle simulation results from several requirements. The models are tested at extreme lift coefficients with possible partial flow separation. In this configuration it is desired to match the dynamic similarity parameters of the test to those of the simulated flight since extrapolation of data to full scale Reynolds numbers is uncertain. Mach number limits, especially in powered models and in tests with rotors, do not permit increasing the test speed beyond that of the simulated free flight. The model must then be increased in size to increase the test Reynolds number.

An additional need to increase the model size is posed by considerations of model design. It is difficult to scale down the elastic modes of a structure with the available material properties. This difficulty is particularly severe in rotor tests which must simulate dynamic response.

Flow distortions due to wind tunnel wall interference may be accounted for if the model tunnel size ratio is small, but the theory becomes less reliable as the model becomes larger [1,2]. In V/STOL vehicle tests with low forward speed and powered lift, the wake of the model is highly deflected. If the tunnel is not extremely large, the wake location will largely deviate from the one in the free air case, and the resulting pitching moment data will be totally different from the real case [3]. The wake may also impinge on the tunnel floor resulting in the development of flow directed upstream along the floor. Lateral recirculation may develop on the walls and flow breakdown will be experienced as reported by Rae [4]. The above reasoning and future projections of testing requirements have encouraged the planning of very large tunnels [5,6].

An alternate or complementary technique to the construction of very large tunnels was developed during this investigation. A wind tunnel is proposed in which the flow is regulated through the walls such that the model in this tunnel is in a flow field like that of free flight during the test. The interference from the

tunnel walls is minimized by active control of the flow through the walls so that correction to the data may not be necessary. This type of wind tunnel is capable of a wider test range than that of the conventional wind tunnel since the flow condition resembles free air flow even for relatively large models at high lift coefficients. In addition, it is not limited to a particular model or geometrical configuration.

The study presents theoretical analysis and experimental evidence in support of this wind tunnel concept. Practical design considerations of flow control and the manner of flow injection are also presented.

SYMBOLS

A	area segment of the tunnel wall
A_H	open area through which the flow is regulated
A_j	jet cross sectional area
AR	aspect ratio
b	model span
$\{B\}$	$M \times N$ matrix of transformation from the model vortex lattice to the tunnel control points
c	model chord
$\{C\}$	$N \times N$ matrix of influence coefficients of the wall vortex elements
C_L	lift coefficient (three dimensions)
C_{ℓ_∞}	free stream lift coefficient
$C_{m_{c/4}}$	moment coefficient at the model 1/4 chord
d	jet diameter
$\{D\}$	$M \times M$ matrix of influence coefficients of the model vortex lattice

E	velocity error due to mass flow mismatch
F	velocity error due to momentum flow mismatch
$\{G\}$	$N \times M$ matrix of transformation from the wall vortex elements to the model boundary points
H	wind tunnel height
i	index of summation
I	identity matrix
$[J]$	M dimensional column matrix defined by Equation (13)
K	dimensionless function defined by Equation (23)
M	number of vortex elements describing a given three dimensional vehicle
m	index of summation
n	index of summation
N	number of vortex elements describing the tunnel geometry
p	index of summation
P	porosity, defined by the ratio of open area to the total area of the wall segment
R	jet radius of curvature
$\{T\}$	$M \times M$ defined by Equation (16)
V	velocity of induced flow near the wall
V_H	controlled flow velocity through the open portion of the wall
V_i	induced velocity at the model control points
V_j	jet velocity
V_∞	free stream velocity
x	streamwise axis with origin at the model 1/4 C the tunnel centerline, positive downstream

4

y vertical axis from the model 1/4 C upward

$[Y]$ M dimensioned column matrix representing the effect of the free stream velocity with appropriate orientation at the vehicle boundary points

α angle of attack

$[\Gamma_{(\ )}]$ M or N dimensioned column matrix of the strengths of the vortex elements

λ eigenvalue

ρ spectral radius of a matrix

ϕ harmonic potential function

Superscript

t wind tunnel parameter

Subscript

o initial arbitrary measurement

w free air condition of the model parameter

THE WIND TUNNEL INTERFERENCE AND PREVIOUS
TREATMENT OF THE PROBLEM

The solution to the wind tunnel interference problem is described using two basic approaches and their combination. The classical approach is to compute the effect of wall interference and then to apply the appropriate corrections to the recorded data. Alternately, by appropriate design, wind tunnels may be constructed with allowance for wall corrections to minimize and in some cases eliminate wall interference.

Although the current development of wind tunnels follows the latter approach, both approaches are briefly outlined here to provide proper perspective for the solution of the problem. A more detailed treatment of previous literature is summarized in two AGARD reports: the first is Agardograph 109 [1] which was prepared in 1966 and the second is AGARD report No. 601 [2] which was published in 1973.

Data Correction

Two Dimensional Wall Interference.-Classically, the constraint imposed by the tunnel walls on the lifting body is described as an effective flow curvature around the model [1,7]. Within the framework of potential flow theory, the effect of the curved streamlines may be replaced by an imaginary camber classically known as aerodynamic camber. Wall effects are approximated by an effective camber proportional to lift coefficient which results in an apparent increase in the lift curve slope.

To correct wind tunnel data the model geometrical angle of attack may be equated to the desired free flight angle and the measured lift may be corrected to the free flight value. Alternately the lift measured in the tunnel may be equated to the free air lift so that the free air angle of attack is equivalent to a corrected angle of attack in the tunnel. Extreme care should be exercised in the use of a classical correction theory for the proper definitions of the correction parameters. Additional discussion on two dimensional wall interference is given in reference [8].

Three Dimensional Wall Interference.-The above discussion may be extended to describe the wall interference in three dimensions. The fictitious aerodynamic camber produced by the walls depends on the location of the model in the tunnel and the size of the

6

model. For a finite wing each wing section would experience different distortion of flow around it. The effect along the span is a continuous apparent camber change or twist as suggested by Heyson [9]. This effect is usually very small in tests of three-dimensional wings.

The most significant effect in three dimensional tests is the upwash due to the images of the trailing vortices which effectively increases the angle of attack at the wing. It produces even a larger upwash at the tail which distorts the pitching moment data. Also the wake behind the model assumes a higher location in the tunnel which further distorts the flow at the tail.

Model blockage provides an additional wall influence. The blockage due to the solid model and its wake induces logitudinal velocity gradients on the uniform flow. This effect, however, is usually quite small in low subsonic testing.

Modern correction theories due to Heyson [2] and Joppa [10] take account of these influences by mathematically including the deflected wake behind the model. By the nature of these approaches data may be corrected only if the distortions due to the walls are relatively small. Practical limit to the applicability of theories is usually considered when the angle of attack correction is less than 5° [2].

Previous Designs of Minimum Interference
Wind Tunnels

Wind Tunnels with Ventilated Walls.-A flight vehicle can be described as supporting its weight by generating a momentum flux through the layers of air stream around it. Each layer with a relative velocity to the vehicle is deflected downward, transmitting a net force upward which supports the flight vehicle.

In a tunnel with rigid walls, the force is transmitted to the model with a much lower downward deflection than the corresponding free flight. In an open tunnel, on the other hand, to provide the same force at the model, the air outside the jet is deflected with a larger angle than in free air.

The opposite effect of closed and open wind tunnels was recognized by Theodorsen [11] who proposed in 1931 several tunnel configurations with open and closed portions to reduce interference. Numerous tunnels with ventilated walls, particularly for transonic testing, have been constructed and are in operation today. The difficulty encountered in using porous or ventilated walls is that

any design is dependent on the model configuration. When a different size model is installed, its relative position in the tunnel varies and so must the desired porosity to minimize the interference.

In addition to problems of configuration dependency, a good theory to correct the data obtained in a ventilated tunnel is not available [1,2,12]. Analytical approaches must deal with discrete boundary conditions. These require no normal flow at the solid portions of the wall and continuous pressure at the slots or open areas.

Mathematically these conditions may be expressed by:

at the solid portion
$$\frac{\partial \phi}{\partial y} = 0 \tag{1}$$

and at the slots the pressure condition leads to

$$\frac{\partial \phi}{\partial x} = 0 \tag{2}$$

Solution to this problem proceeds by introducing either a porosity or a slot parameter so that the boundary conditions may be transformed to homogeneous boundary conditions [1]. The applicability of this approach and the relation between the porosity parameter and the physical structure is still to be resolved [2,12].

A more recent development proposes to incorporate active elements on the wind tunnel wall so that the tunnel may accommodate an arbitrary model configuration.

Wind Tunnels with Active Walls.-The desire to obtain minimum interference wind tunnels with semi-active walls was documented in experimental work by Kroeger, et al. [13]. The method employed adjustable wall louvers. Partial success of the technique was summarized in the final report of that investigation [14]. However, analytical foundations for further design of such a tunnel have not been published.

Another proposal for a porous wind tunnel with forced draft through the walls was prepared by Hall and Gamage [15]. Numerical analysis was made for the required flow through the wall.

8

During the preparation of this study some work on minimum correction wind tunnels was published by the staff of the Calspan [16,17]. Their proposal calls for the use of a comparison between two flow components in order to evaluate the flow improvement in the tunnel. The method is based on the fact that in plane potential flow the two velocity components are not independent. Therefore, one of the two measured flow components is used to compute the second velocity component. The computed velocity is then compared with the corresponding measurement. Experimental data to evaluate that proposal are not yet available.

Additional work was reported to be underway by Ferri, et al. [18]. That study was initiated in transonic wind tunnels and it would attempt to measure the pressure and streamline deflection near the ventilated walls. Comparisons of measured pressure and deflection with those computed by analytical models would be used to change the wall porosity.

OBJECTIVES OF THE STUDY

The present development of minimum correction wind tunnels employs active flow control through the tunnel walls. The amount of flow to be regulated through the wind tunnel surface is computed by potential theory and is based on the actual lift measured on the model. The choice of the particular potential flow model will depend on the intricacy of the flight vehicle and the relative size of the tunnel.

The main objective of this investigation was to demonstrate the feasibility of the minimum interference wind tunnel. The pertinent questions in the design of such a wind tunnel were evaluated analytically and experimentally.

The discussion in this report is addressed to the following questions:

(a) Show that in principle it is possible to obtain a minimum correction wind tunnel by controlling the flow at the walls.

(b) Analyze an appropriate way to regulate the flow through the walls.

(c) Develop a principle of operation for an arbitrary lifting body.

(d) Assess practical considerations to be used in the construction of an active wall wind tunnel.

THEORETICAL ANALYSIS

Analytical Considerations

The basic assumption of the active wall wind tunnel is that potential flow analysis provides an accurate description of the flow far away from the model. While the detailed structure of the flow may vary widely with the aerodynamic body very close to that body, it approaches that of the simple horseshoe vortex model in a short distance.

This description is supported by experimental evidence. The familiar wake of a contra-rotating vortex pair has been documented for a wide variety of lifting bodies. A reference is made to works by Heyson, et al. [10] which illustrates experimentally that the wake behind a helicopter rotor blade is rolled up into a vortex pair at seven percent of the blade radius behind the rotor. This pattern is reproduced in Fig. 1.

In accordance with the above discussion, at some distance from the model (i.e., near the wind tunnel walls) a fictitious control surface may be constructed. On this control surface potential theory is applicable in an arbitrary wind tunnel and for an arbitrary aerodynamic body. In particular, it is recalled that the solution to the potential flow problem is unique. Therefore, if at every point on the control surface the flow is identical to that of free air, the model inside the control volume will experience free flight flow. The applicability of potential theory to this physical problem then provides a theoretical basis for constructing a minimum correction wind tunnel.

A practical consequence of the potential theory is that it is sufficient to control only the normal component of the flow on the boundary. This result is due to the fact that a potential function (in this case the free air potential of the model) is uniquely defined by its normal derivative on the control surface (assuming the potential to vanish at infinity) (See, for example, [20].).

The principle of operation for the proposed wind tunnel is as follows. Starting with an arbitrary model and configuration, the lift is measured. Potential theory is utilized with a simple flow model to compute the required flow conditions along the wall. This computed flow is then provided by injection or extraction. Because such flow modifications change the lift, a continuous feedback occurs as is illustrated in Fig. 2.
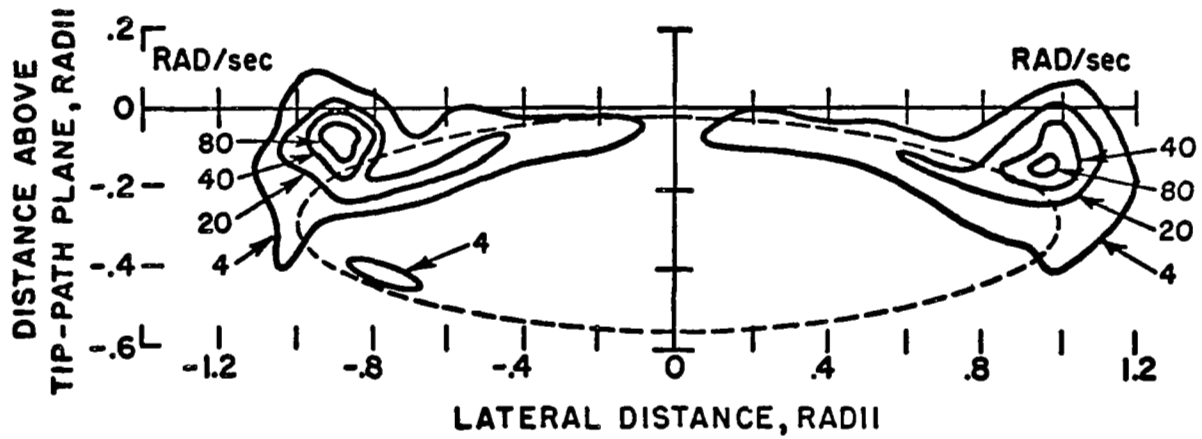
10

Figure 1. Vorticity distribution at seven percent of radius behind a helicopter rotor (NACA TR 1319).
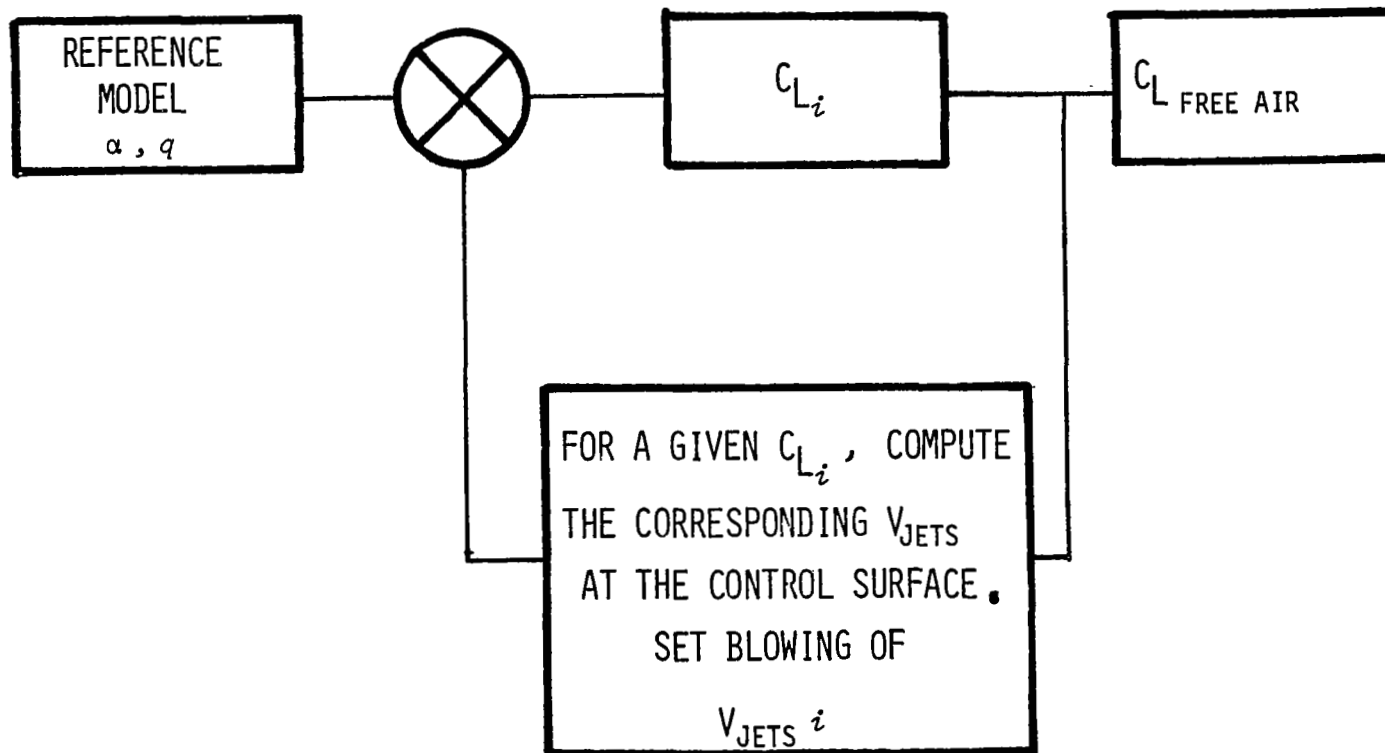
Figure 2. Feedback model of the minimum correction wind tunnel.

It is now necessary to prove that this process converges and the measured lift will assume the free air value. The proof is presented for the general three dimensional problem, and is repeated for the two dimensional case.

Generalized Three Dimensional Theory.-The discussion of the general theory is based on the feedback concept in Fig. 2. For any given tunnel it will be necessary to use a potential flow model to compute the necessary flow through the wall. The feedback path will be obtained in reality by a new measurement of the lift.

In this analytical treatment the feedback mechanism is also modeled by a potential model which enables one to prove that the process is convergent.

The potential flow field for any arbitrary model may be constructed by any desired number of M elements representing a proper vortex lattice description and any combination of horseshoe vortices as illustrated in Fig. 3.

The boundary conditions of no flow through the body surface and the Kutta condition are satisfied at M points. It is given by the following tensor relation:

$$\{D\}[\Gamma_w] = (Y) \qquad (3)$$

where D is the matrix of influence coefficients having $M \times M$ dimensions. It represents the effect of all the body elements at each of the control points.

The free air circulation is analogous to the lift coefficient representation in Fig. 2. The column matrix Y of M dimensions represents the free air velocity and any desired body orientation which is given by an angle of attack, a side-slip angle or a roll angle. Γ_w then represents the flight vehicle in free air.

Any arbitrary wind tunnel may be constructed in principle by choosing a sufficient number of vortex rings, N, to construct a wall of vortex lattice as proposed by Joppa [10]. The wind tunnel boundary condition of no flow through the wall is satisfied at the N control points on the wall. The velocity induced by the model is equated with the velocity due to all the vortex rings which form the tunnel walls. In a wind tunnel with active wall, the wall effect is related to the instantaneous value of circulation desig-
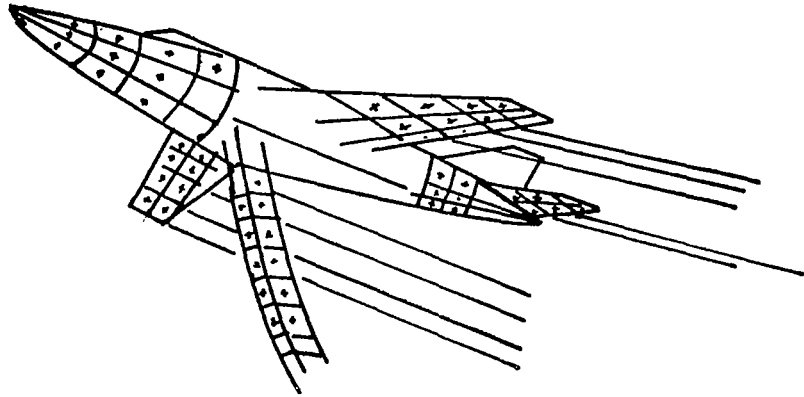
POTENTIAL FLOW REPRESENTATION

$$\{D\}\left[\Gamma_W\right] = \{Y\}$$

Figure 3.   Potential flow representation
            for a general three dimensional
            vehicle.

14

nated by the $i + 1$ step. The wall boundary condition is given by:

$$\{C\}\left[\Gamma^t\right] = \left[V_m{}^t{}_{i+1}\right] \tag{4}$$

where the $N \times N$ matrix C is the influence coefficient matrix of the velocity contributions of all the vortex rings at each control point. Γ^t is an N dimensioned column matrix and $V_m{}^t{}_{i+1}$ is the velocity due to the model. Fig. 4 is an illustration of the problem.

The velocity induced by the model on the wall control points is given by the following N equations:

$$\left[V_m{}^t{}_{i+1}\right] = \{B\}\left[\Gamma_{i+1}\right] \tag{5}$$

Combining equations (4,5) to solve for the strength of the vortex lattice elements will result in:

$$\left[\Gamma^t{}_{i+1}\right] = \{C\}^{-1}\{B\}\left[\Gamma_{i+1}\right] \tag{6}$$

Consequently, the velocity contribution of the wind tunnel on the model is given by:

$$\left[V_{wall_{i+1}}\right] = \{G\}\left[\Gamma^t{}_{i+1}\right] \tag{7}$$

where the $N \times M$ matrix, G, represents the influence of the tunnel vortex elements at the M model boundary points. $V_{wall_{i+1}}$ is an M dimensions column matrix.

A similar representation may be constructed for the induced flow by the active control system. The controlled flow on the wall is based on the previous measurement of lift at the ith step. The induced flow at the M model boundary points due to the active
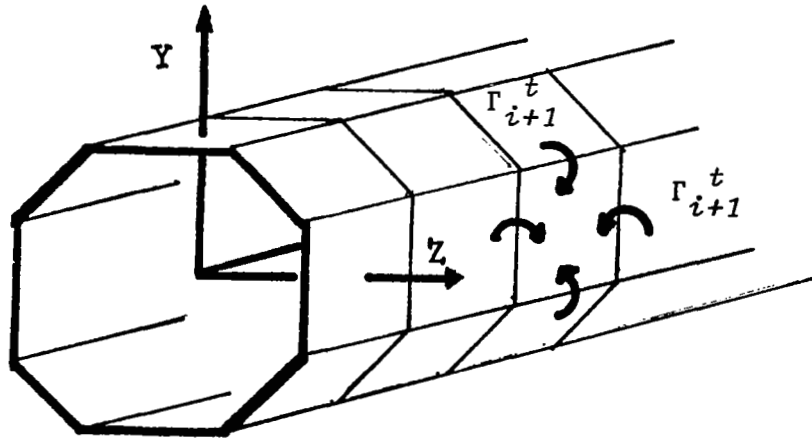
THE WIND TUNNEL PROBLEM

$$\{C\}\left[\Gamma_{i+1}^{t}\right] = \{B\}\left[\Gamma_{i+1}\right]$$

CONTROLLED FLOW

$$\{C\}\left[\Gamma_{i}^{t}\right] = \{B\}\left[\Gamma_{i}\right]$$

Figure 4. Vortex lattice representation of a wind tunnel.

16

wall is given by:

$$\left[V_{jets_i}\right] = \{G\}\left[\Gamma_i{}^t\right] \qquad (8)$$

Equation (6) may be substituted into Equations (7) and (8) (with the proper i index) so that the flow due to the wall and the flow due to the active wall will be expressed in terms of the model circulation.

$$\left[V_{wall_{i+1}}\right] = \{G\}\{C\}^{-1}\{B\}\left[\Gamma_{i+1}\right] \qquad (9)$$

and

$$\left[V_{jets_i}\right] = \{G\}\{C\}^{-1}\{B\}\left[\Gamma_i\right] \qquad (10)$$

The mathematical analogy which represents the effect of the active wall wind tunnel may be reconstructed by summations of all velocity influences in the field at the model M boundary points.

$$\{D\}\left[\Gamma_{i+1}\right] - \{G\}\{C\}^{-1}\{B\}\left[\Gamma_{i+1}\right] + \{G\}\{C\}^{-1}\{B\}\left[\Gamma_i\right] = [Y] \qquad (11)$$

Equation (11) may be rearranged to separate the M dimensioned column matrix Γ_{i+1}.

$$\left[I - \{D\}^{-1}\{G\}\{C\}^{-1}\{B\}\right]\left[\Gamma_{i+1}\right]$$
$$= \{D\}^{-1}\{Y\} - \{D\}^{-1}\{G\}\{C\}^{-1}\{B\}\left[\Gamma_i\right] \qquad (12)$$

In order to prove the convergence of the feedback model, the problem may be restated as follows: It is necessary to prove that the iterative relation given by Eq. (12) will solve the unique potential flow problem given by the free air model

$$\{D\}\left[\Gamma_w\right] = \left[Y\right] \tag{3}$$

This problem is similar to problems of convergence encountered in numerical analysis [21]. It is convenient to define an M dimensioned column matrix J which represents the difference between the instantaneous value of the circulation and the free air circulation.

$$\left[J_i\right] = \left[\Gamma_i\right] - \left[\Gamma_w\right] \tag{13a}$$

$$\left[J_{i+1}\right] = \left[\Gamma_{i+1}\right] - \left[\Gamma_w\right] \tag{13b}$$

Equation (12) may be rearranged with the aid of Eq. (3)

$$\left[\Gamma_{i+1}\right] - \left[\Gamma_w\right] = \{D\}^{-1}\{G\}\{C\}^{-1}\{B\}\left\{\left[\Gamma_{i+1}\right] - \left[\Gamma_i\right]\right\} \tag{14}$$

Equations (13a,b) may be introduced into Eq. (14). After simplification, the result is given by:

$$\left[J_{i+1}\right] = (-1)^i\{T\}\left[J_i\right] \tag{15}$$

where

$$\{T\} = \left[I - \{D\}^{-1}\{G\}\{C\}^{-1}\{B\}\right]^{-1}\{D\}^{-1}\{G\}\{C\}^{-1}\{B\} \tag{16}$$

Then the circulation measured in the wind tunnel will converge to the free air value if the difference between the two, J, will vanish. For m iterations J is expressed by:

$$[J_m] = (-1)^m \{T\}^m [J_o] \qquad (17)$$

Mathematically it is necessary to show that T is convergent, i.e.,

$$\lim_{m \to \infty} \{T\}^m = \{0\} \qquad (18)$$

where $\{0\}$ is a zero matrix

A necessary and sufficient condition for the convergence of T is for the spectral radius of T to be less than one [21].

$$\rho(T) = \max_M \left| \lambda_M \right| < 1 \qquad (19)$$

In general it may be difficult to compute the eigenvalues, λ_m, due to the complexity of the matrix T. An equivalent condition to the convergence of T is for any matrix norm of T to be less than 1. This condition is illustrated by the following.

$$\max_i \sum_{j=1}^{M} \left| T_{ij} \right| < 1 \qquad (20a)$$

or

$$\max_j \sum_{i=1}^{M} \left| T_{ij} \right| < 1 \qquad (20b)$$

where T_{ij} are understood to be the elements of T.

In the wind tunnel problem the matrix T relates the geometries of the model to those of the tunnel. The range of the relative sizes of the tunnel and models for which the system converges will have to be analyzed with specific configurations. When this study is carried out, attention should be given to possible reduction of matrix size due to physical symmetry.

On the basis of two examples, presented in the Appendix, the conditions for the convergence of T are not expected to present any practical limitation on the use of a given tunnel. In a two dimensional case which is discussed further in the next section, it was found that the condition for convergence is satisfied even for wind tunnels whose height is equal to the model chord. In the second example of the Appendix, computed values for a simplified, three dimensional case demonstrate that the feedback model is generally convergent. Specific designs, however, will have to be studied in more detail.

Two Dimensional Approach.-As discussed above, the analysis is described as a stepwise process, although in practice it may be continuous. The steps are designated by the index i and each one contains two paths as illustrated in the feedback model in Fig. 2. In the forward path the lift is measured in a given configuration of the model, angle of attack and the wind tunnel dynamic pressure. The lift coefficient, C_{ℓ_i} is used to compute the appropriate jets of the active wall system. In the feedback path, the controlled flow is introduced at the wall. The lift on the model is changed and a new value of lift coefficient, $C_{\ell_{i+1}}$ will be measured.

The analytical relation between the new lift coefficient $C_{\ell_{i+1}}$ to the lift coefficient of the previous step, C_{ℓ_i}, is described as follows: The flight vehicle is represented by a simple vortex at its quarter chord, and its boundary condition is satisfied at its 3/4 chord. The normal velocity at that point is the sum of velocities due to each influence in the field as illustrated in Fig. 5. These are the velocity due to the wing itself and the normal component of the free stream as is usually done in the free air case. In the presence of the wind tunnel walls a third component represents the effect of the walls. This flow component can be calculated by the method of images in the usual way. A fourth velocity component which is introduced at the model 3/4 chord results from the flow through the tunnel walls. This latter flow is regulated at will through the wall. The sum of these velocities is given by the following:
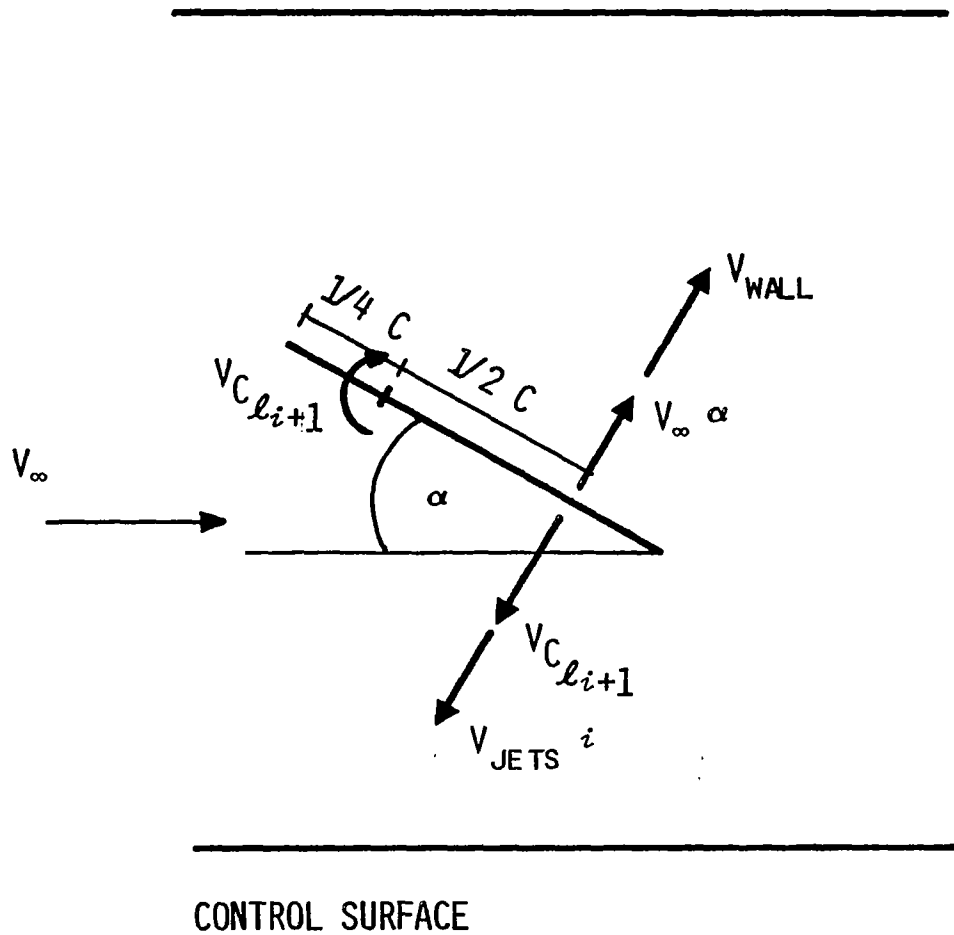
CONTROL SURFACE

Figure 5. Mathematical analogy of the minimum
interference wind tunnel in two
dimensions.

$$V_{C_{\ell_{i+1}}} + V_{jets_i} - V_{wall} = V_\infty \alpha \qquad (21)$$

It should be noted that the index of the velocity induced by the model is $i + 1$ while the jets at the wall were computed on the basis of the previous value of lift coefficient in the ith step.

Using the method of images, it may be shown that the velocity induced by the walls on the 3/4 chord point is given by the following:

$$V_{wall} = C_{\ell_{i+1}} \frac{V_\infty}{2\pi} K \qquad (22)$$

where the function, K, represents the sum of the infinite number of images which satisfy the boundary condition at the wall. K may be computed by

$$K = \frac{1}{2} \left(\frac{C}{H}\right) \sum_{p=1}^{\infty} (-1)^{p+1} \frac{C/H}{\left(\frac{C}{2H}\right)^2 + p^2} \qquad (23)$$

The controlled flow through the surface is made to match the flow due to the model that would exist at the wall proximity in free air. It may be calculated mathematically by images outside the tunnel. The flow induced by the wall jets at the model 3/4 chord is given by:

$$V_{jets_i} = C_{\ell_i} \frac{V_\infty}{2\pi} K \qquad (24)$$

Substituting Eqs. (22) and (24) into Eq. (21) and expressing the velocity induced by the model in terms of the lift coefficient results, after simplification, in:

$$C_{\ell_{i+1}} = \frac{2\pi\alpha}{1 - K} - C_{\ell_i} \frac{K}{1 - K} \qquad (25)$$

This recursion relation does not necessarily imply a discrete process rather than a continuous one but it is introduced as a convenient device to prove the convergence of the technique. For n iterations Eq. (25) may be written as:

$$
c_{\ell_n} = \frac{2\pi\alpha}{1 - K} \left[1 - \left(\frac{K}{1 - K} \right) + \left(\frac{K}{1 - K} \right)^2 - \cdots \right] +
$$

$$
+ (-1)^n c_{\ell_o} \left[\frac{K}{1 - K} \right]^n \tag{26}
$$

This alternating geometrical series converges to the free air value of $2\pi\alpha$ provided that the function K is less than one half. Simple calculation will show that this is indeed the case when the ratio of model chord to tunnel height is less than 1.

It is of interest to note that in this theoretical model, given an initial value of lift coefficient and an error bound on the desired accuracy, one may compute the number of iterations necessary to to obtain the approximate free air lift coefficient. Even in a continuous-testing facility the number of iterations may be related to the required run time to obtain the free air condition. Such an analysis of course depends on the particular design and configuration.

This proof applies to the ideal case where the injection is continuously distributed. Both mass flow and momentum across the control surface will then be matched with free air conditions to obtain a perfect simulation.

Practical Considerations

In practice the flow is injected through discrete holes in the wall so that, if the mass flow is matched over an area, its momentum is greater than that of the ideal case. Alternatively, the integral of the momentum of the ideal flow through the surface may be equated to the momentum through the discrete holes resulting in a mass mismatch. The ratio given by the area of the holes in the porous walls to the total area of the wall will be henceforth referred to as porosity. It follows that the design of a minimum correction wind tunnel may be constructed on the principle of either momentum flow matching or mass flow matching.

23

Momentum Flow Matching.-A minimum correction wind tunnel may be designed to match the momentum flow. In this case the momentum through each segment of the wind tunnel surface is equated to the momentum flow through the porous area of that segment. Consequently, a deficiency of mass flow would result and the force on the model would be undercorrected. As the wall porosity increases the mismatch between the mass flow and the momentum flow will decrease.

In each segment, the momentum matching may be expressed mathematically by:

$$\int V_H{}^2 d\, A_H = \int V^2\, d\, A \qquad (27)$$

where V is the velocity through the wall in the free air case and V_H is the velocity in the active wall through the open area.

If each segment is sufficiently small the flow velocity that would exist in free air throughout the segment location is approximately constant. Equation (27) may then be evaluated as follows:

$$V_H{}^2 A_H \cong V^2\, A \qquad (28)$$

then

$$V_H \cong V\, P^{-1/2} \quad \text{for} \quad P > 0 \qquad (29)$$

where P is the wall porosity.

Consequently, in order to obtain momentum flow matching the flow at each segment is regulated to match V_H of Eq. (29).

The expected error in measured lift as a function of both the porosity and the model chord to tunnel height ratio is given by the following approximate analysis.

The error associated with a practical design of an active wall wind tunnel may be expressed in terms of the mass flow deficiency when the momentum flow is matched. At some distance from the wall the mass flow deficiency may be expressed as a continuous velocity field:

24

$$\int E \left(\frac{C}{H}, P\right) dA = \int V \, dA - \int V_H \, dA_H \qquad (30)$$

This integral relation is correct when the flow does not reverse its direction throughout the segment. Using the earlier assumption that each segment is small and substituting Eq. (29) into Eq. (30) will result, after simplification, with the following:

$$E \left(\frac{C}{H}, P\right) = V[1 - P^{1/2}] \qquad (31)$$

Equation (31) expresses a measure of the velocity error that exists at some distance from the wall.

E represents the velocity difference near the tunnel wall between the desired flow for a perfect simulation and the existing flow at a given porosity. When the porosity approaches unity (i.e., 100 percent of properly regulated flow) the velocity error vanishes as expressed in Eq. (31). E equals the velocity induced by the wall when the porosity vanishes. For these reasons E may replace the velocity due to the wall and that due to the controlled flow which were used in the ideal case of the previous analytical section.

The contributions to the velocity error from all the wall segments may be provided mathematically by a vortex lattice analogy similar to the controlled flow representation of the active wall in the previous section. With appropriate transformation, G, the effect of the velocity error near the wall may be introduced at the M vehicle boundary points. The measured lift on the body for a given porosity may be computed by the following matrix relation:

$$\{D\}[\Gamma] - \{G\}[VE] = [Y] \qquad (32)$$

where VE is an N dimensional column matrix representing the velocity error at each vortex ring which is defined by Eq. (31). The circulation computed by Eq. (32) provides the expected lift in an active wall wind tunnel with a given porosity.

25

A two dimensional case may be simply analyzed as follows:
The simple flow analogy of a vortex at the $C/4$ point and the body
boundary condition at $3/4$ C may be used to approximate the effect
of this velocity error on the measured lift. Figure 6 illustrates
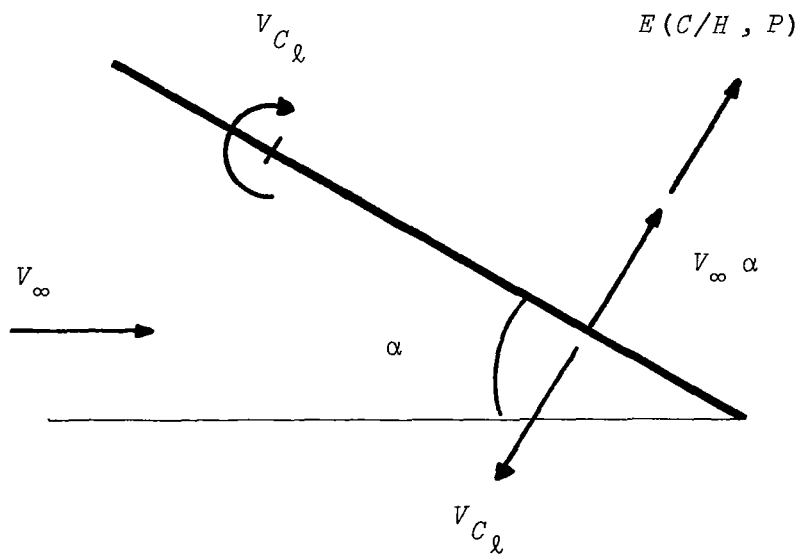the flow model of interest.

Figure 6. Mathematical model of two dimensional
wall interference as a function of porosity.

For small angle of attack the velocity sum at $3/4$ C point is given
by:

$$V_{C_\ell} - E\left(\frac{C}{H}, P\right) = V_\infty \alpha \qquad (33)$$

Expressing the velocity, V, on the right hand side of Eq. (31) in
terms of the wall images given in Eq. (22) results in the following
relation:

26

$$E\left(\frac{C}{H}, P\right) = C_\ell \frac{V_\infty}{2\pi} \left[1 - P^{1/2}\right] K \qquad (34)$$

Substituting Eq. (34) into Eq. (33) and expressing the induced velocities in terms of the lift coefficient gives, after simplification, an expression for the change in lift in the tunnel:

$$\frac{C_\ell}{C_{\ell_\infty}} = \frac{1}{1 - [1 - P^{1/2}] K} \qquad (35)$$

It should be pointed out again that Eq. (35) satisfies two limiting cases of porosity. When the porosity approaches zero (corresponding to a closed wall wind tunnel), Eq. (35) is reduced to the classical approximate wall interference relation [1]. When the porosity approaches unity, the corresponding physical case is a perfect control of every point on the control surface and the measured lift approaches the free air value.

Mass Flow Matching.-In this approach, the surface of the tunnel is divided into segments, each of which is made to match the mass flow that would exist in the absence of walls. The momentum injected or extracted through each segment will be larger than that of free air. The excess momentum causes an overcorrection to the measured force on the model. This effect is similar to that observed in open wind tunnels in which the momentum wake deflects through a larger angle than that of free air.

The computed mass flow through each wall segment is regulated through separate plenum chambers behind the individual segment. While the amount of mass flow is independent of the porosity, lower values of porosity would produce jets with increasingly higher momentum and the associated larger interference.

The flow error analysis may follow similar logic to the one used in defining the error for momentum flow matching. In this case, however, there is an apparent excess mass flow through the wall which corresponds to the excess momentum in the porous area.

Consequently, in each wall segment the excess mass flow over the amount that will produce a momentum match may be expressed by:

27

$$\int F\left(\frac{C}{H}, \ P\right) \ dA = \int V_H dA_H - \int V \ dA \qquad (36)$$

The general error analysis then proceeds in a similar way to the one presented for momentum matching. For a two dimensional case the lift interference is given by:

$$\frac{C_\ell}{C_{\ell_\infty}} = \frac{1}{1 - [P^{1/2} - 1] \ K} \qquad (37)$$

It is apparent in this simplified analysis that when the mass flow is matched the measured lift will be lower than that which is measured in free air.

Wall Jets.-As an additional note to the analytical study, the mechanism of injection and extraction of flow through the control surface is reviewed. While flow extraction may be sufficiently represented by a mathematical analogy of a sink [22], injection of flow may not be represented by a potential model of a source. A difference in the physical phenomena is apparent by the following example: the human body would suffocate in its sleep if inhaling would have been the true inverse of exhaling.

Injection of flow in the minimum correction wind tunnel may be described as the introduction of normal jets into a uniform flow. This subject was the topic of numerous papers [23,24], but remains an open question to date.

The extensive experimental investigation on normal jet into a uniform flow indicates three regions in the jet trajectory. At the initial stage the shape of the cross section is approximately preserved. In the next region, the jet is highly curved and its cross section is distorted into a kidney shape. Finally, the jet cross section rolls into a vortex pair and the jet appears to approach the direction of the uniform flow.

The governing parameters are:

(1) Pressure effects from the uniform flow on the jet are significant in bending the jet in the preliminary stages.

(2) Fluid from outside the jet is entrained by viscous

mixing on the periphery of the jet wake. This
mechanism appears to be significant in the
shaping of the jet trajectory.

(3) Vorticity is generated on the jet boundary which
rolls up into a vortex pair.

Analytical treatment of the problem necessitates a description
of the entrainment and pressure mechanisms which appear to have a
significant effect on the jet trajectory. Attempts to solve the
problem to date have relied on semi-empirical techniques. A widely
accepted empirical jet trajectory due to Margason [25] was used in
the selection of the jet diameter for the experimental study. The
analysis assured that the wall jets would not hit the model.

For the purpose of the active wind tunnels, two areas of
interest were reviewed.

The displacement effect of the incoming jets was modeled by a
potential flow analogy of a source. It was found, however, that
displacement effects at the proximity of the wind tunnel center were
negligible.

When the pressure forces on a jet are equated to the centri-
fugal forces, it is possible to compute an effective circulation
which is generated at the jet. This approach was suggested by
Wooler [26] and the circulation is given by:

$$\frac{\Gamma}{V_\infty} = \left(\frac{V_j}{V_\infty}\right)^2 \frac{A_j}{Rd} \qquad (38)$$

The radius of curvature of the jet was computed using Marga-
son's empirical relation. The calculations showed, however, that
the vorticity effects on the far field (i.e., in the vicinity of
the model) are negligible for the jet velocity and jet diameter in
the active tunnel system.

The implication of the above discussion is that flow injection
should be through a large number of small jets which will result
in a relatively low ratio of jet velocity to free stream velocity.
This design would limit the region of turbulent viscous mixing to
the wall proximity.

EXPERIMENTAL STUDY

Design Considerations

Experimental evaluation of the concept was carried out utilizing a two dimensional model for its simplicity. Injection and extraction through the walls were carried out with a pattern of holes so that the active wall jets were three-dimensional.

Consequently, the method of flow control through porous walls is identical to that which would be implemented in a three dimensional tunnel while the necessary corrections are simple. In this case, two dimensional tests provide a more direct approach than three dimensional tests to investigate design parameters represented by the concepts of mass matching and momentum matching and the effect of porosity on such a wind tunnel.

A construction of a wind tunnel with adjustable floor and ceiling permitted the variation of the tunnel height from twelve times the chord to twice the chord. The variation of the tunnel height represents two limiting cases. The one case with tunnel height of twelve times the chord may be taken as a close approximation to free flight conditions, while the latter case of tunnel height equal to twice the model chord represents an extremely small tunnel. Such a tunnel is probably smaller than that which would be used for practical research work.

The controlled flow requirement was computed by a simple potential flow model. For this two dimensional experiment the necessary amount of flow through the wall was on the order of four percent of the tunnel flow. The amount of flow would depend of course on the exact model configuration and lift coefficient.

The advantage of the variable height wind tunnel to study the concept of minimum correction wind tunnel is that all the necessary apparatus is self-contained. The model is placed in effectively the same experimental facility to provide approximate free air data, distorted data due to wall constraints in a small tunnel, and finally the data of the proposed new wind tunnel. The same model, instrumentation and Reynolds' number were used in all study stages.

30

Test Setup and Procedure

A prototype minimum correction wind tunnel was constructed by installation of movable floor and ceiling in an 8 × 1 (ft × ft) subsonic wind tunnel. A sketch of this tunnel is given in Fig. 7. The same airfoil model was used throughout all the experimental tests. The model used had an eight inch chord.

Initial tests were run in the original tunnel having a height of twelve times the chord. With the installation of the movable floor and ceiling the model was in a small tunnel with height of two model chords.

The flow quality in terms of pressure gradients and flow angularities was evaluated in the tunnel at each stage of the investigation. Measurements were made in the original tunnel using static pressure ports at one foot intervals along the floor and ceiling of the tunnel. Additional static ports were spaced vertically at two stations approximately seven model chords upstream and downstream from the model. A tube with static pressure ports at one foot intervals was installed along the tunnel center line. To eliminate any errors due to misalignment in the tube, its position was varied so that each pressure reading was repeated with several static ports at the same spatial locations. A dynamic pressure gradient of eight percent was found to exist in the loft length of the original (8 × 1) tunnel.

An appropriate boundary layer allowance was designed and confirmed for the tunnel inserts. The inserts could be rotated to taper the top and bottom of the small tunnel. Static ports were installed at one half foot intervals on the floor and ceiling of the small tunnel. Pressure data from these locations indicated that in the final installation no velocity gradients were present along the streamwise axis of the tunnel.

Studies with boundary layer probe showed the wall boundary layer on each wall to be less than four percent of the tunnel width at the model station in the tunnel.

The tunnel dynamic pressure was found to have periodic fluctuations. This is believed to be the result of a poor diffuser which exhibits periodic flow separation and re-attachment. Special care was taken to monitor the dynamic pressure at the time of data recording. For each configuration ample run time was allowed to observe steady state conditions and to assure consistency of data recording. Several runs were made at each configuration and significant departures of mean flow parameters due to dynamic pressure surges were discarded.
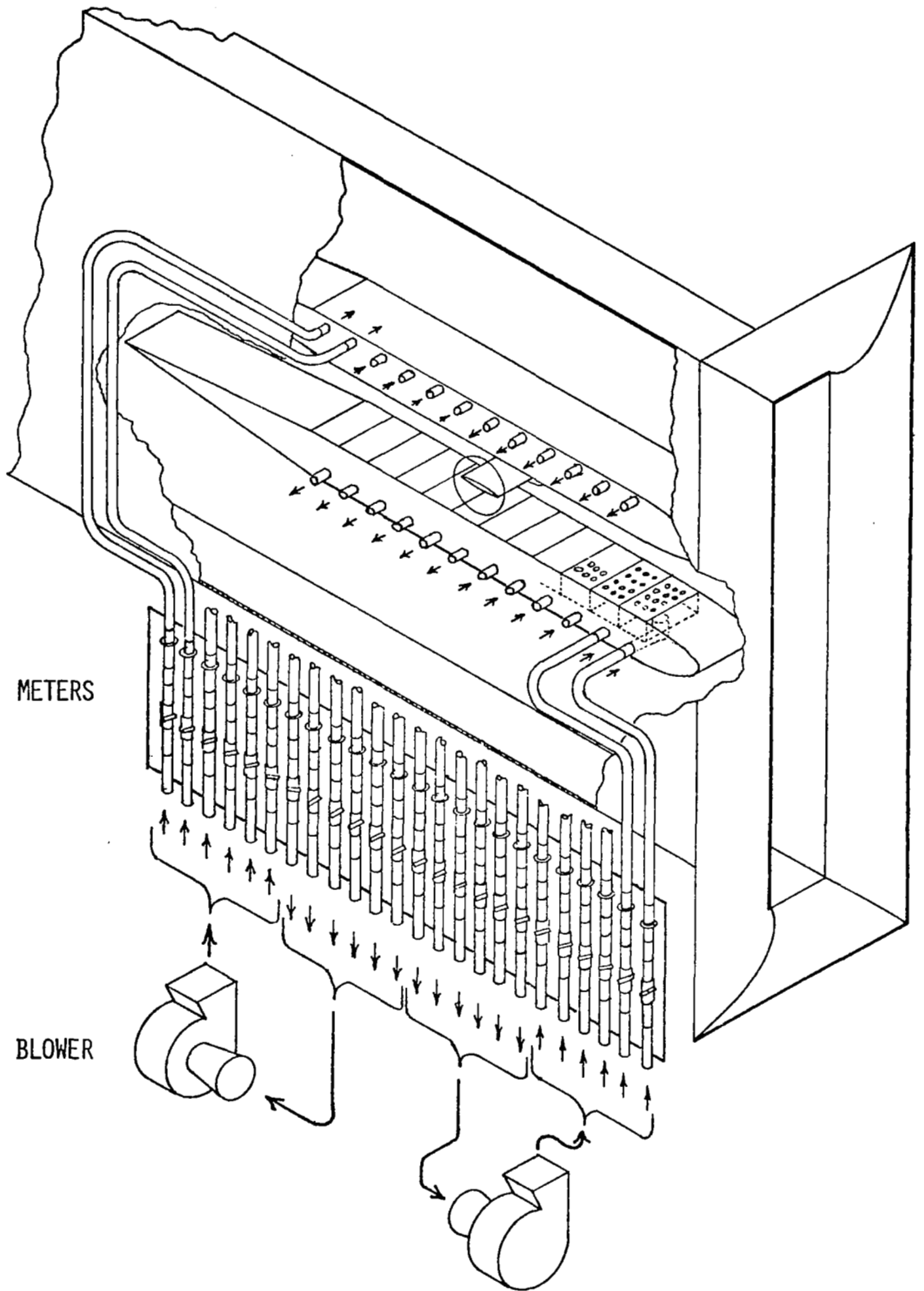
METERS

BLOWER

Figure 7.   Schematic of the minimum
            interference wind tunnel.

For the active wall wind tunnel the control surface extended four and one-half model chords upstream and four and one-half model chords downstream from the model. This is illustrated by the controlled segments of the floor and ceiling in Fig. 7. Twenty-four plenum chambers were used to regulate the flow through the surface.

The porous plates which cover each plenum chamber were removable so that the porosity could be varied by installation of an appropriate set of plates.

The flow into or from each plenum chamber was generated by two blowers. The flow was controlled by manual values and monitored with flow meters.

For the prototype wind tunnel used in this study, adjustment of flow in one line was reflected in flow changes of the rest of the flow lines connected into the same blower. Two to three complete iterations of valve adjustments were necessary to obtain the desired flow condition for each model configuration.

For the active tunnel portions of the test, the proper amount of blowing was set using the free air potential model for the given wind tunnel dynamic pressure and the actual lift measured on the model. Then the flow through the active wall was held constant while the model angle of attack was varied through ten angle increments. This procedure provided a range of lift values on the model for a constant injection rate. The results of these tests for a given configuration of active walls were analyzed for data consistency. The data of interest were the ones in which the active wall system was set in accordance with the actual model lift. The lift coefficient for a given angle of attack was adjusted in a few cases to conform with the family of runs for a constant active wall setting. This technique reduced the possibilities of error in the active wall data.

Smoke was utilized as a spot check to assure that the jet mixing region was confined to the far field with respect to the model.

Initial tests were made with tunnel wall porosity of five percent and later tests were made with wall porosity of approximately thirty-one percent.

Lift data was taken utilizing chordwise pressure taps at the midspan of the model. Data were photographically recorded and punched into cards after each run. Reduction of data and data analysis was performed by a digital computer. In order to integrate the pressure data polynomials were fitted numerically to the discrete data points. Polynomials of several (up to fifth order) were used to assure the accuracy of the final integration.

Tests were run with a dynamic pressure of twelve pounds per square foot at a Reynolds' number of 0.4×10^6. The model used was a symmetrical airfoil section NACA 65A015.

Active Wall Instrumentation.-As outlined above, the flow through the wall was distributed through twenty-four plenum chambers. Manual valves were designed to obtain good flow control in each of the twenty-four lines. Control was provided by rotation of a disc in the flow line with provisions to lock the disc when a desired flow was achieved.

Orifice type flow meters were designed in accordance with ASME standards. The diameter ratio between the orifice opening to the pipe was 0.65. Each flow meter was individually calibrated. The calibrating unit was a venturi shaped pipe with a pitot tube at its throat. The velocity profile was assumed to be flat at the throat so that the volume flow (assuming incompressible and irrotational flow) through the calibrating unit could be predicted. The calibrating unit was installed in each flow line to obtain the volume flow as a function of pressure variation through the orifice type meters. A typical calibration curve is given in Fig. 8. The variations between the calibration curves of the various meters were small, however each individual calibration curve was used in the tests.

RESULTS AND DISCUSSION

Results of the experiments are presented in the form of lift curves for various model to tunnel height ratios and injection rates. Injection rates range from complete mass flow matching to momentum flow match.

Several hundred configurations and reruns were made to assure repeatability. The results presented here will be given in a summary form only. Figure 9 illustrates the pressure distribution on the model for an angle of attack of approximately 5.0 degrees. Model chord to tunnel height ratio of 0.08 represents the original tunnel, which is taken as an approximate free air flow. The ratio of 0.5 reflects the data in the small tunnel having a height of twice the chord.

Pressure data were integrated to construct Fig. 10 which is a plot of the lift curve slope in the large and small tunnel. The classical increase in the lift curve slope was produced. It should be noted that at this low Reynolds' number, the linear portion of the curve is very short. Measurement of the slope would depend on the linear approximation to the curve. The change in the lift slope is on the order of 12 percent, while according to the linear
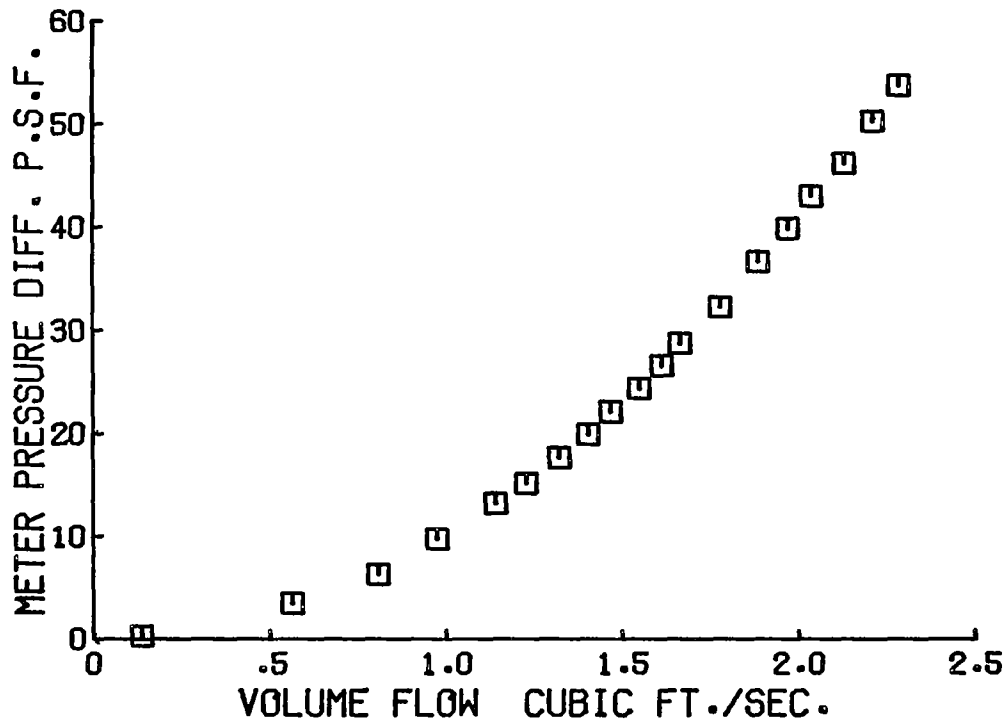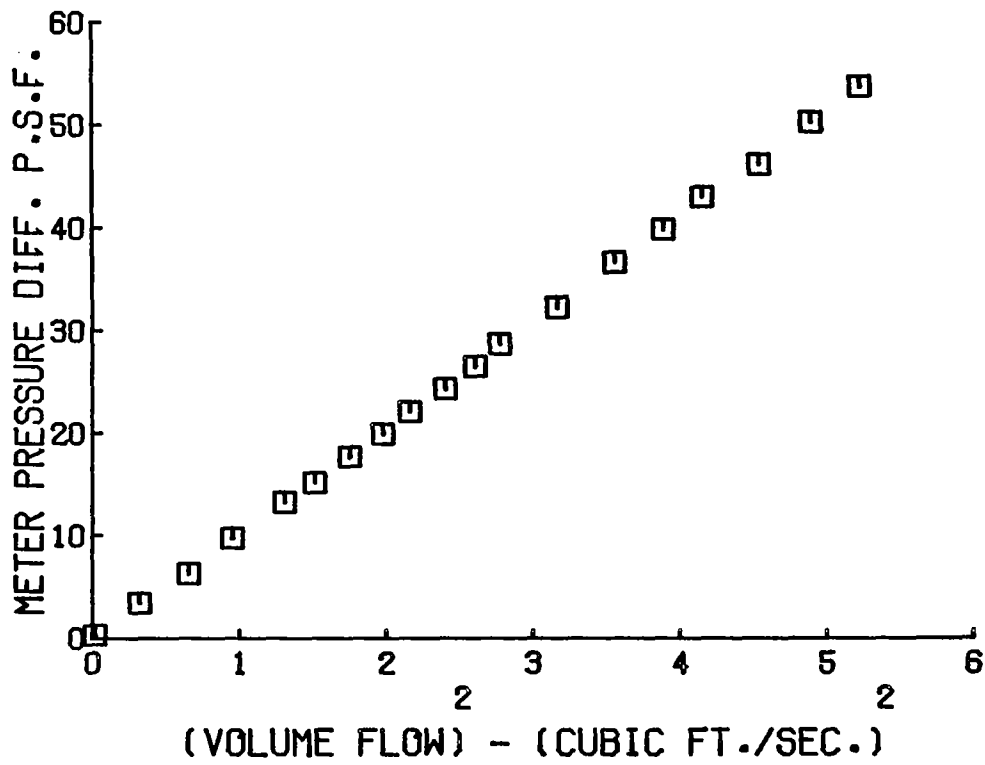
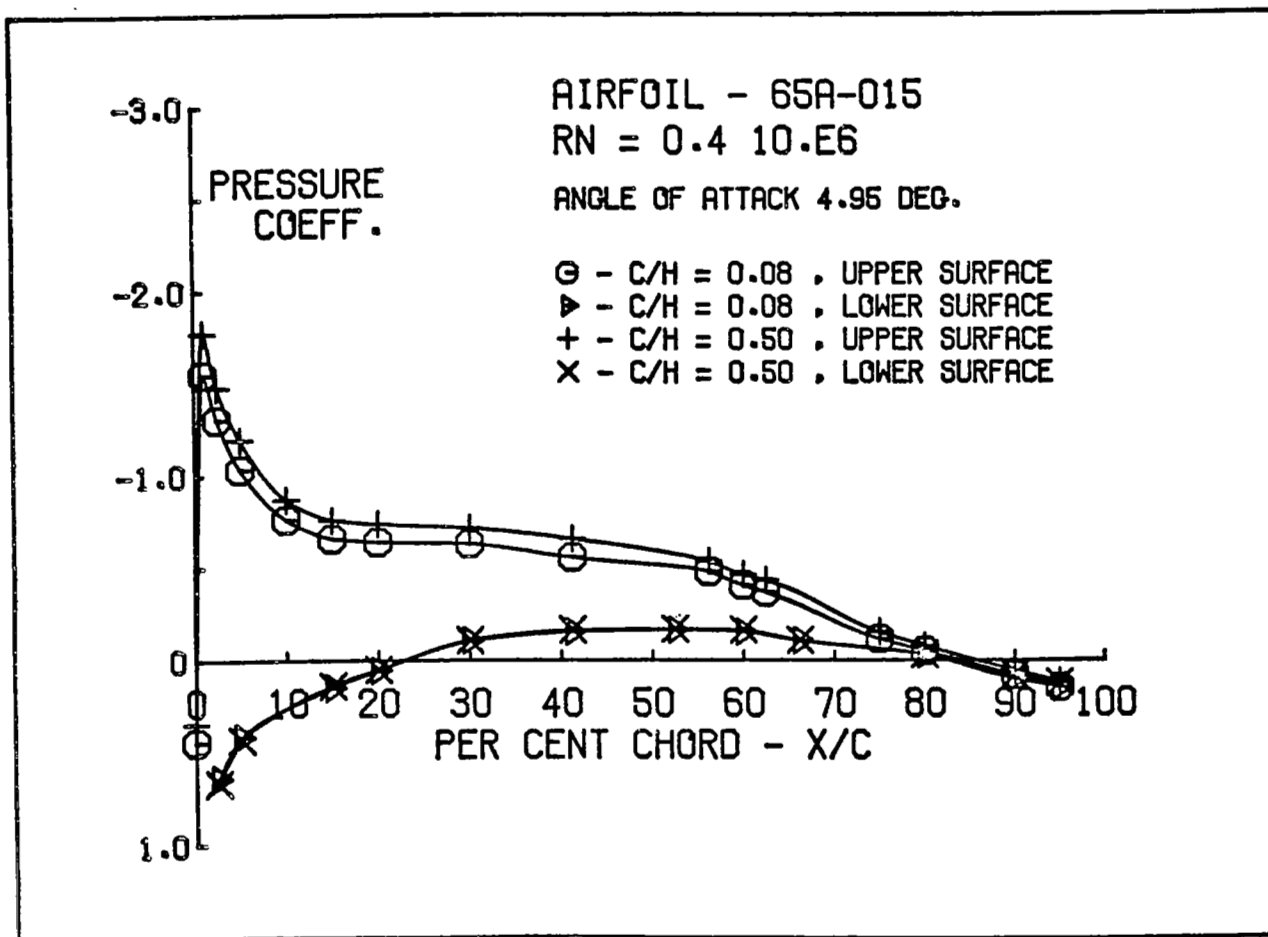Figure 8.   Typical flow meter calibration curve.

Figure 9. Model to tunnel ratio effect on airfoil pressure
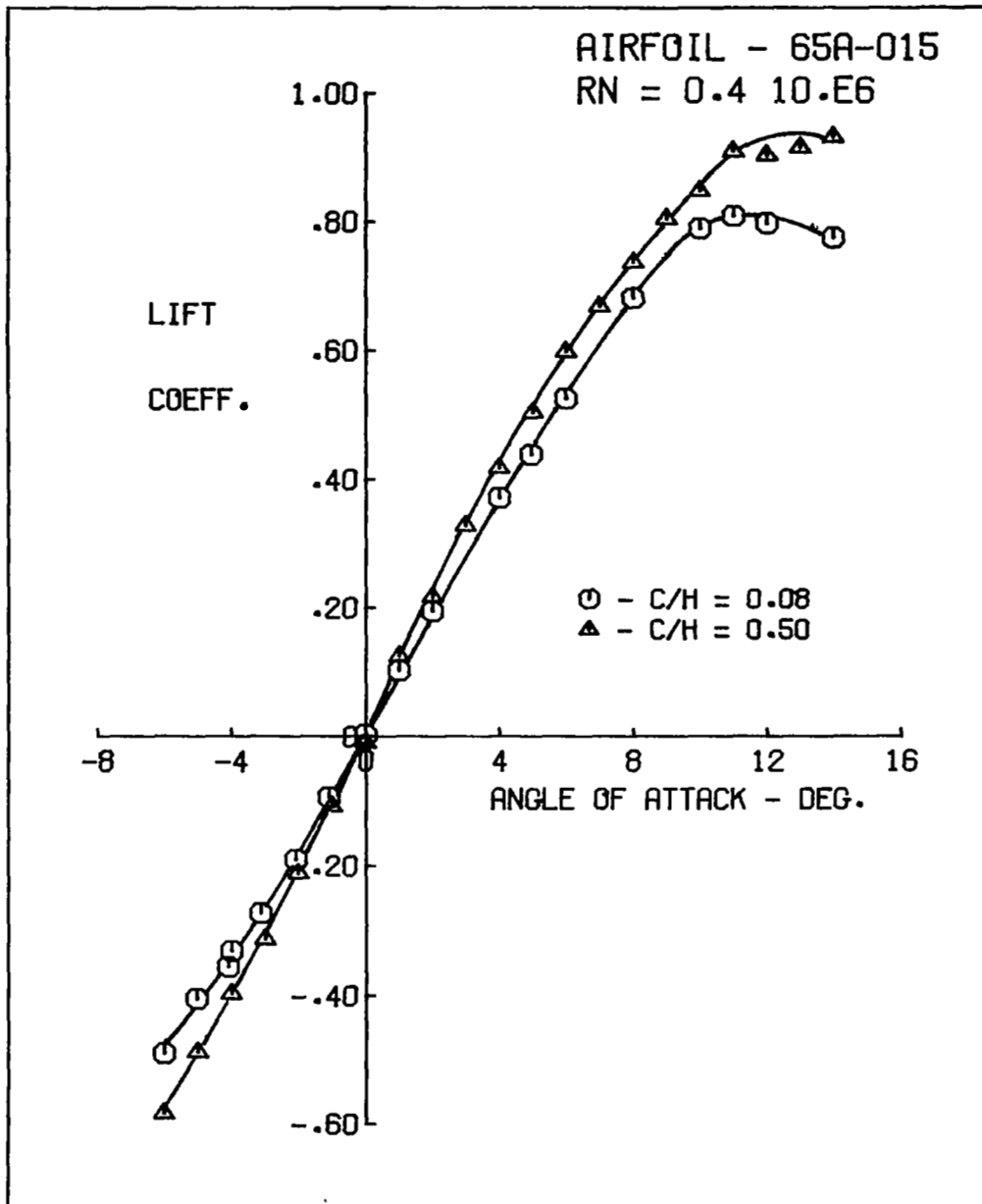distribution.

Figure 10.   Lift interference in a two
dimensional wind tunnel.

interference theories discussed earlier [1] the change in the lift slope should be approximately 10 percent.

Before proceeding to discuss the results of the active wall wind tunnel, a sample of smoke pictures is presented. Figure 11 includes two smoke photographs showing the region near the airfoil. The porosity for this case was thirty-one percent. It can be seen qualitatively that the flow in the model vicinity is well ordered.

The region at which turbulent mixing starts is shown in Fig. 12.

In Fig. 12a the smoke is relatively thin indicating ordered flow, while in Fig. 12b the smoke line is thick, which implies turbulent mixing. For this case the mixing region height is approximately seven jet hole diameters from the wall.

A summary of model configurations using five percent porosity is given in Fig. 13. The mass principle causes an overcorrection because of large momentum mismatch while momentum match undercorrects the flow. It is important to note that even at such a low value of porosity, the data indicate a significant departure from data of the closed wall small tunnel. Similar observation is made for the data obtained with wind tunnel wall porosity of approximately thirty-one percent as illustrated in Fig. 14. These data were substantiated by considerable evidence of additional unpublished results.

As the porosity increases, a decrease is observed in the difference between lift curves obtained with momentum matching.

The rate of flow improvement in the tunnel may be illustrated by plotting the change in slope as a function of porosity. This analysis is summarized in Fig. 15. The figure includes a plot of the error analysis given by Equations (35,37). The experimental data agree quite well with the theoretical prediction based on the simple linear theory. The bracket symbols in Fig. 15 were obtained by computing the lift ratios at several angles of attack so that they represent the range of actual measurements.

CONCLUSIONS AND RECOMMENDATIONS

The results of the investigation demonstrate both theoretically and experimentally the utility of this concept in wind tunnels.

Theoretical analysis supports the philosophy of constructing a minimum correction wind tunnel using active walls. The analytical study substantiates the convergence of flow conditions in the tunnel to those of free air using the lift as a measure of the flow im-
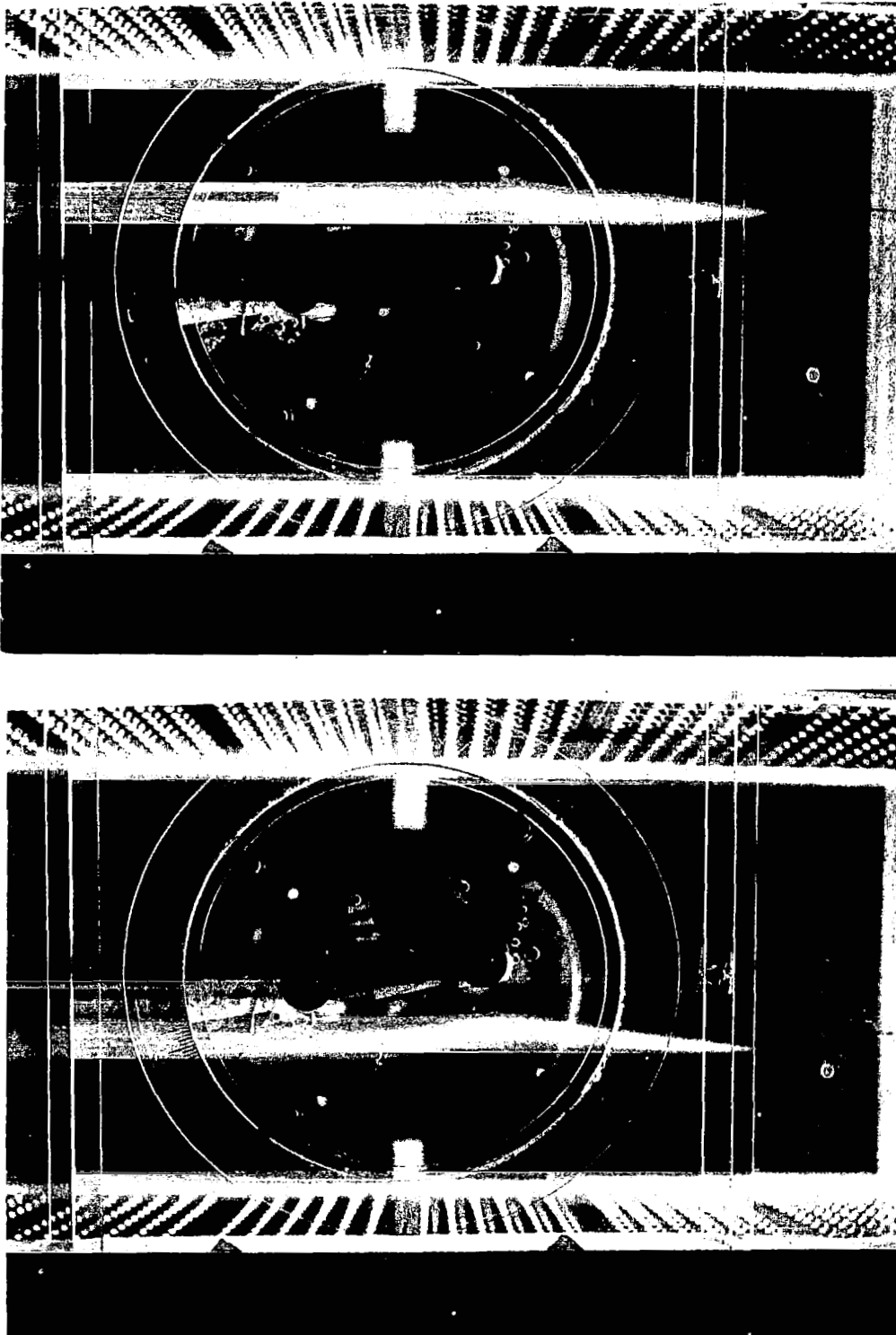
Figure 11. Flow around an airfoil using momentum matching in a minimum interference wind tunnel.
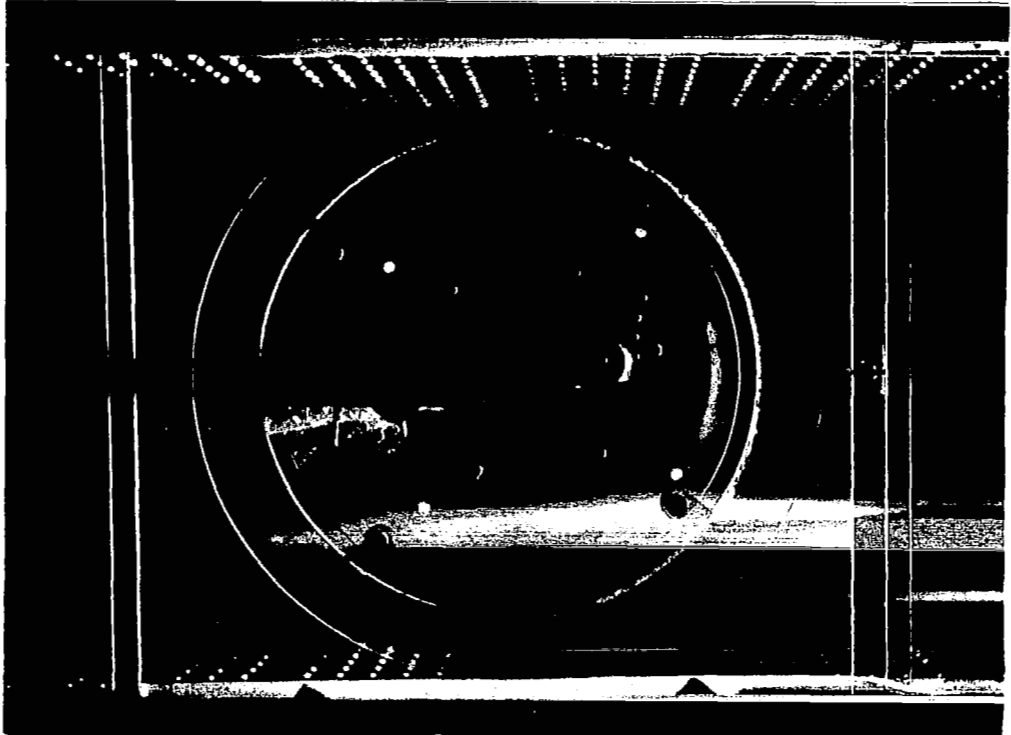
Figure 12.   Mixing region of injected flow in a
             minimum interference wind tunnel.

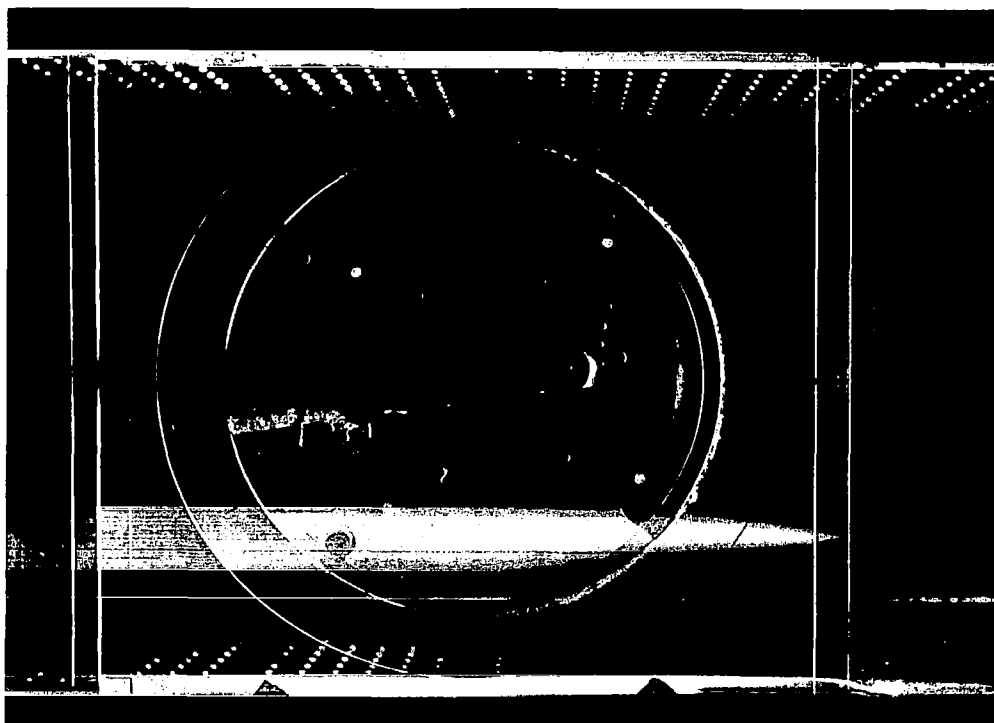(A)   Smoke nozzle at $0.28H$ from the tunnel floor.

40

Figure 12. Mixing region of injected flow in a
minimum interference wind tunnel.
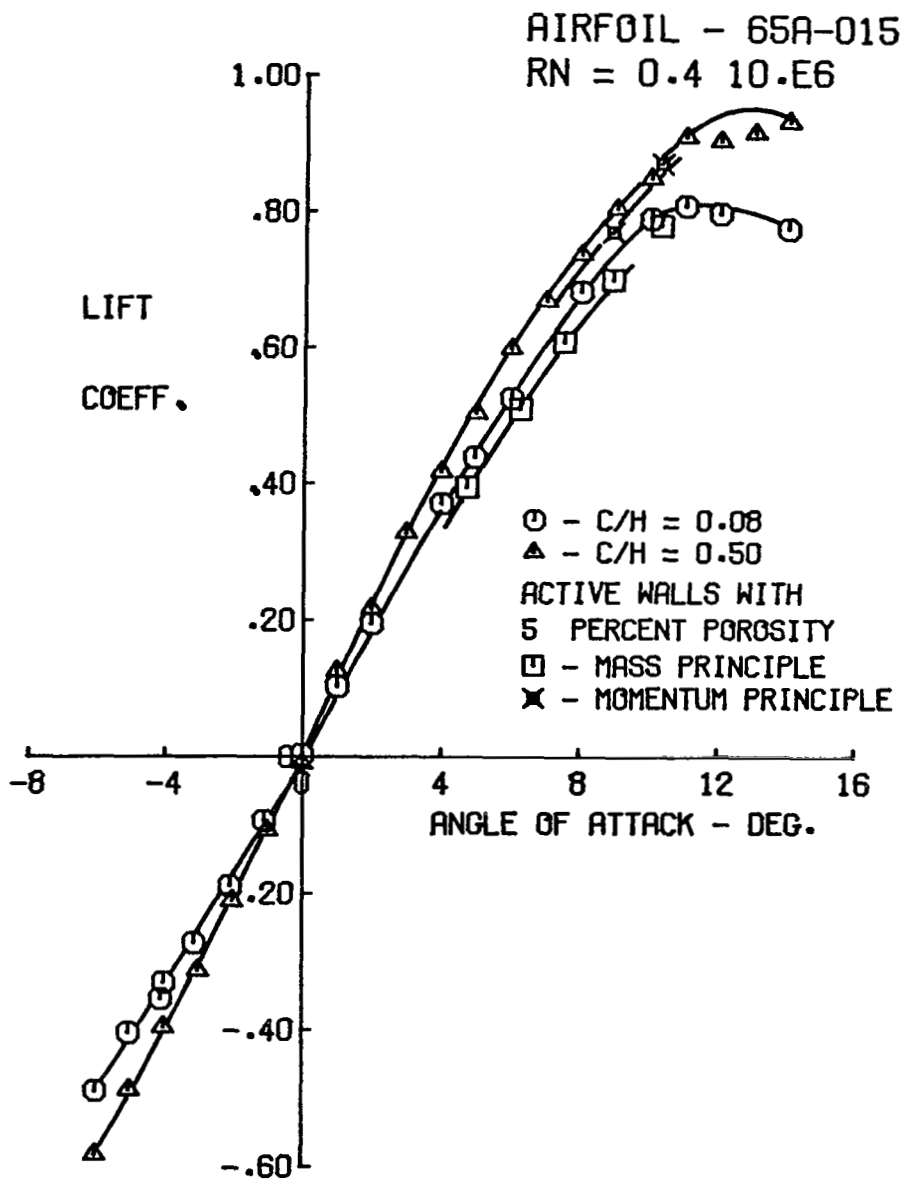
(B) Smoke nozzle at $0.24H$ from the tunnel floor.

Figure 13. The effect of active walls with 5% porosity on the lift interference in a two dimensional tunnel.
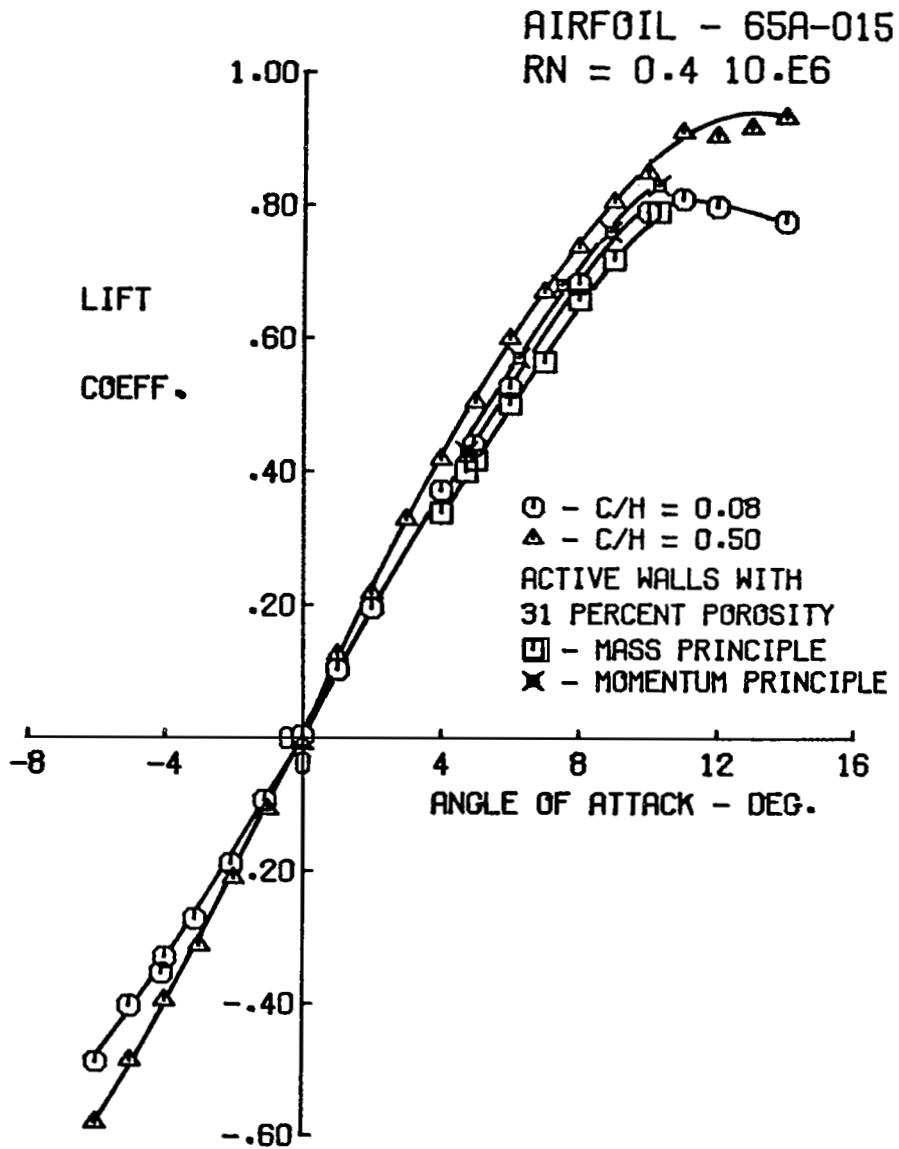
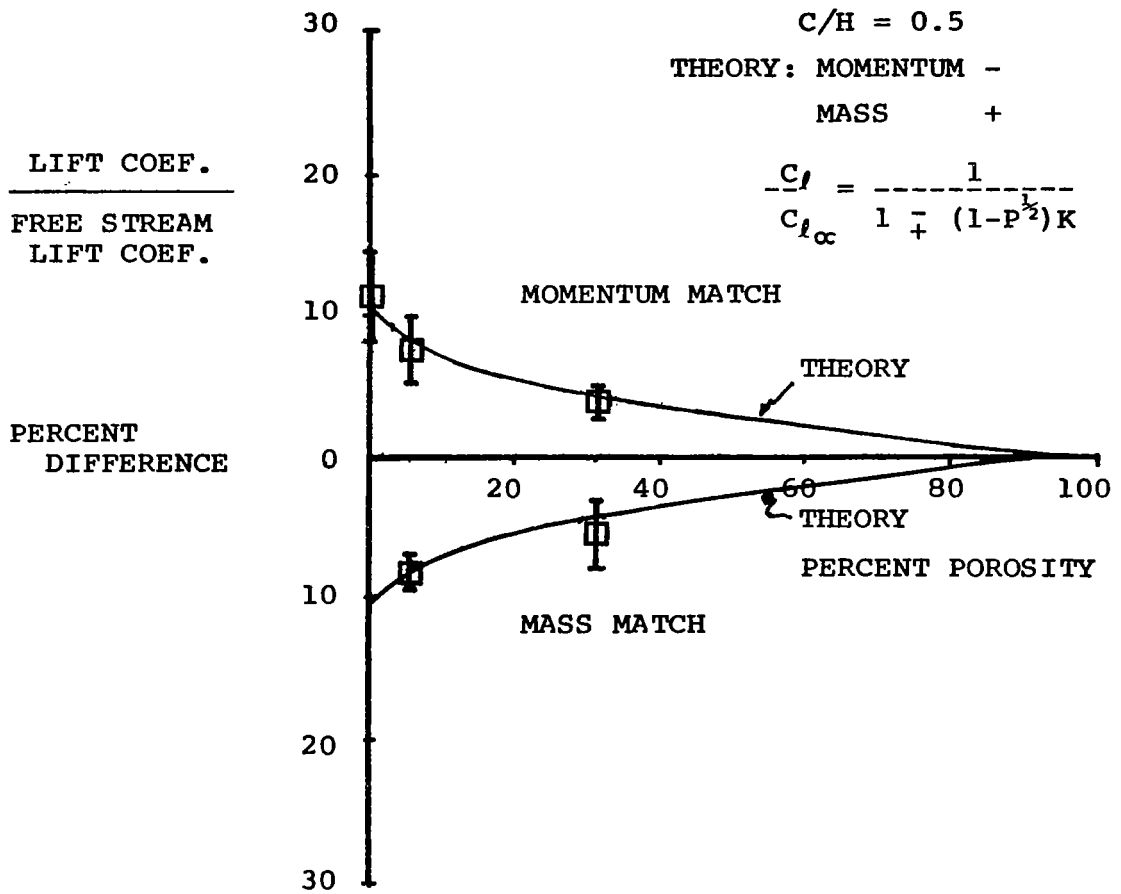Figure 14. The effect of active walls with 31% porosity on lift interference in a two dimensional wind tunnel.

Figure 15. Active wall effectiveness as
a function of porosity.

44

provement. Of practical interest is the theoretical conclusion that it is necessary to control only the flow normal to the wall surface of the tunnel.

When the design is based on matching mass flow, the excess momentum causes an overcorrection; when momentum is matched, the mass flow is deficient so that the lift curve is undercorrected. The difference between the two cases decreases rapidly as the porosity increases.

In this study both extreme cases of matching either mass or momentum were investigated. This approach was desired for the analysis of the concept in principle. For practical construction of a research wind tunnel, flow control may be based on a combination of both momentum and mass requirements for an optimum facility.

It should be emphasized that the amount of injected or extracted flow through the walls was only on the order of four percent of the total flow in the small wind tunnel. The amount of controlled flow through the wall will be higher in three dimensional tests or for tests of models with active elements; however, its percentage of the total mass flow will be inversely proportional to the tunnel size.

The results obtained in this work indicate that a minimum correction wind tunnel may be achieved with relatively low porosity of active walls. An exact value of porosity would depend on the accuracy requirements; however, the interference was substantially reduced with approximately thirty percent wall porosity.

Recommendation for further study on the concept of minimum interference may be followed on several topics.

A study may be pursued on the effect of reduction in the number of controlled plenum chambers. For that study, a high degree of experimental accuracy will be required. Quantitative assessment of introducing flow into the tunnel will add to the refinement of the theory for the minimum interference wind tunnel.

A second topic of concern is a design problem of an automated system for the feedback control loop. Stability investigation for such a system should be analyzed particularly for possible limit cycles. An additional subject of interest is the time required for convergence. While in subsonic wind tunnels the test time is not a severe limitation, application of the concept to transonic flow simulation will require appropriate modifications for extremely short run times.

The flow field was theoretically described in this report with an overview, macroscopic analysis. This approach was satisfactory for the introduction and demonstration of the concept. Eventually,

the refinement of the technique will require a more exact description of the flow field, including the relative influence of each plenum chamber and injection jet.

A final recommendation on the basis of this study is to implement this approach in three dimensional wind tunnels.

REFERENCES

1. Garner, H. C., Rogers, E. W. E., Acum, W. E. A., and Maskell, E. C., *Subsonic Wind Tunnel Wall Corrections*, Agardograph 109, 1966.

2. Carbonaro, Mario, "Review of Some Problems Related to the Design and Operation of Low Speed Wind Tunnels for V/STOL Testing," in *Problems in Wind Tunnel Testing Techniques*, AGARD Report No. 601, April 1973.

3. Heyson, H. H., *The Effect of Wind Tunnel Wall Interference on the Performance of a Fan-in-Wing VTOL Model*, NASA TN D-7518, February 1974.

4. Rae, W. H., Jr., "Limits of Minimum-Speed V/STOL Wind Tunnel Tests," *Journal of Aircraft*, Vol. 4, No. 3, May-June 1967, pp. 249-254.

5. Templin, R. J., "Recent Trends in Low Speed Wind Tunnel Design and Techniques," in *International Congress on Subsonic Aeronautics*, ed. T. L. Hall, *Annals of the New York Academy of Sciences*, Vol. 154, Art. 2, November 1968, pp. 1055-1073.

6. Kelly, M. W., Mort, K. W., and Hickey, D. H., *Full-Scale Subsonic Wind Tunnel Requirements and Design Studies*, NASA TM X-62, 184, September 1972.

7. Garner, H. C., *Note on Aerodynamic Camber*, Aeronautical Research Council, R. & M. 2820, 1950.

8. Bernstein, S., *The Minimum Interference Wind Tunnel*, Ph.D. Dissertation, University of Washington, Department of Aeronautics and Astronautics, March, 1975.

9. Heyson, H. H., "Wind Tunnel Wall Effects at Extreme Force Coefficients," in *International Congress on Subsonic Aerodynamics*, ed. T. L. Hall, *Annals of the New York Academy of Sciences*, Vol. 154, Art. 2, November 1968, pp. 1074-1093.

10. Joppa, R. G., *Wind Tunnel Interference Factors for High-Lift Wings in Closed Wind Tunnels*, NASA CR-2191, February 1973.

11. Theodorsen, T., *The Theory of Wind Tunnel Interference*, NACA Report 410, 1931.

12. Parkinson, G. V., and Lim, A. K., "On the Use of Slotted Walls in Two-Dimensional Testing of Low Speed Airfoils," *Canadian*

Aeronautics and Space Institute Transactions," Vol. 4, No. 2,
September 1971, pp. 81-87.

13. Kroeger, R. A., and Martin, W. A., *The Streamline Matching Technique for V/STOL Wind Tunnel Wall Corrections*, AIAA Paper 67-183.

14. Kroeger, R. A., *Wind Tunnel Design for Testing V/STOL Aircraft in Transition Flight*, Arnold Engineering Development Center, AD 749154, September 1972.

15. Hall, D. G., and Gamage, R. W., *Principles of Reducing Boundary Interference at Subsonic Speeds Using a Forced Draft, Porous-Wall Wind Tunnel*, Northrup Corporation, NOR-70-96, April 1970.

16. Sears, W. R., "Self Correcting Wind Tunnels," *Aeronautical Journal*, February/March 1974, pp. 80-89.

17. Erickson, J. C., Jr., and Nenni, J. P., *A Numerical Demonstration of the Establishment of Unconfined-Flow Conditions in a Self-Correcting Wind Tunnel*, CALSPAN Report RK-5070-A-1, 1973.

18. Ferri, A., and Baronti, P., "A Method for Transonic Wind-Tunnel Corrections," *AIAA Journal*, Vol. 11, No. 1, January 1973, pp. 63-66.

19. Heyson, H. H., and Katzoff, S., *Induced Velocities Near a Lifting Rotor with Non-Uniform Disk Loading*, NACA Report 1319, 1957.

20. Courant, R., and Hilbert, D., *Methods of Mathematical Physics*, Vol. II, Interscience Publishers, New York, Third Printing, July 1966.

21. Isaacson, E., and Keller, H. B., *Analysis of Numerical Methods*, John Wiley and Sons, Inc., New York, 1966.

22. Batchelor, G. K., *An Introduction to Fluid Dynamics*, Cambridge at the University Press, 1970.

23. *Analysis of a Jet in a Subsonic Cross Wind*, a Symposium held at Langley Research Center, Hampton, Virginia, September 1969, (NASA SP-218).

24. Skifstad, J. G., "Aerodynamics of Jets Pertinent to VTOL Aircraft," *Journal of Aircraft*, Vol. 7, No. 3, May-June 1970, pp. 193-204.

25. Margason, R. J., *The Path of a Jet Directed at Large Angles to a Subsonic Free Stream*, NASA TN D-4919, 1968.

26. Wooler, P. T., "On the Flow Past a Circular Jet Exhausting at Right Angles from a Flat Plate or Wing," *Journal of the Royal Aeronautical Society*, Vol. 71, March 1967, pp. 216-218.

APPENDIX

EVALUATION OF CONVERGENCE REQUIREMENT

FOR PARTICULAR CONFIGURATIONS

The principle of operation for the minimum interference wind tunnel guarantees that the measured lift in the tunnel will approach the free air value provided that the matrix T converges. T is expressed by:

$$[T] = \left(I - \{D\}^{-1}\{G\}\{C\}^{-1}\{B\}\right)^{-1}\{D\}^{-1}\{G\}\{C\}^{-1}\{B\} \qquad (A1)$$

where the description of the matrices on the right hand side of Eq. (A1) is given in the general theory section of this study.

Evaluation of the norm of T may become tedious for a detailed test geometry. Two simple examples are presented here.

Example 1: Two Dimensional Tunnel

The model is represented by a single vortex so that the dimension of T is 1×1. Because of the symmetry of the problem it is convenient to represent the wall by a single valued vortex element equal to the sum of the wall images. Consequently, the dimension of C is 1×1. It can easily be shown that in this case all the matrices in Eq. (A1) have a single dimension.

Finally the norm of T is less than one provided that the following scalar relation is preserved:

$$\frac{GB}{DC} < \frac{1}{2} \qquad (A2)$$

49

where G, B, D, C are the single elements of the corresponding matrices. $\{C\}$ and $\{B\}$ may be evaluated using the boundary condition at the tunnel wall.

$$\{C\} = \{B\} = \frac{1}{2\pi H} \left\{ \frac{\frac{x}{H}}{\left(\frac{x}{H}\right)^2 + \frac{1}{4}} \right\} \tag{A3}$$

$\{G\}$ is the transformation of the images' effect at the model 1/4 chord. It may be expressed by

$$\{G\} = \left\{ \frac{1}{2\pi} \frac{C}{H^2} \frac{\pi^2}{12} \right\} \tag{A4}$$

$\{D\}$ is the influence coefficient of the vortex at the 3/4 chord point.

$$\{D\} = \left\{ \frac{1}{\pi C} \right\} \tag{A5}$$

Substitution of Eq. (A3) through (A5) into Eq. (A2) provides the condition for the convergence of T in terms of the model chord to tunnel height ratio.

$$C/H < 1.102 \tag{A6}$$

Example 2:   Simple Square Wind Tunnel

The model is given by a single horseshoe vortex placed at the model 1/4 chord and the tunnel is constructed by four vortex rings. The problem of interest is illustrated in Fig. Al.

For this case only, the normal velocity components are of interest. Because of physical symmetry it may be argued that the two vortex rings representing the side walls are of zero strength and the top and bottom vortex rings have equal strength.
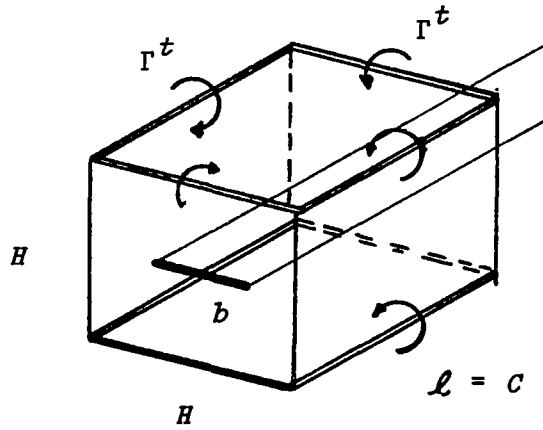
Figure A1:   Mathematical model of
a simple square tunnel.

For this case only the normal velocity components are of interest.   Because of physical symmetry it may be argued that the two vortex rings representing the side walls are of zero strength and the top and bottom vortex rings have equal strength.

Following symmetry considerations it is also possible to show that each component of T in Eq. (A1) has a single dimension as was the case in the previous example.

To facilitate the computation the length of the vortex ring and consequently the length of this wind tunnel is equated to the model chord.   The results of this analysis then may be taken only as illustrating the technique rather than being accurate computations.

The functional form of the elements in Eq. (A1) for this case are presented as follows:

$$\{B\} = \frac{1}{\pi b} \left\{ 1 + \frac{\frac{b}{H}\left(1 + AR^2\right)}{AR\left[\left(\frac{b}{H}\right)^2\left(1 + \frac{1}{AR}\right) + 1\right]^{1/2}} \right\} \tag{A7}$$

51

$$\{C\} = \frac{\frac{b}{H}}{\pi b} \left\{ \frac{1}{\left[1 + \left(\frac{b}{H\ AR}\right)^2\right]^{1/2} \frac{b}{H\ AR}} + \right.$$

(A8)

$$+ \frac{\frac{b}{H\ AR}}{\left[4 + \left(\frac{b}{H\ AR}\right)^2\right]\left[5 + \left(\frac{b}{H\ AR}\right)^2\right]^{1/2}} + \frac{2}{5\left[\left(\frac{b}{H\ AR}\right)^2 + 5\right]^{1/2}} \left. \right\}$$

$$\{D\} = \frac{1}{\pi b} \left\{ 1 + \frac{1 + AR[1 + AR^2]^{1/2}}{1 + AR^2} \right\}$$

(A9)

$$\{G\} = \frac{2}{\pi b} \frac{b}{H} \left\{ \frac{\left[\frac{b}{H\ AR} + 1\right]^2}{\left[\left(\frac{b}{H\ AR}\right)^2 + 1\right]\left[4 + \left(\frac{b}{H\ AR}\right)^2\right]^{1/2}} \right\}$$

(A10)

These equations were obtained by modifications of the general equations for a horseshoe vortex and vortex rings. (Formulation of these equations was presented by Joppa, R. G., *Wind Tunnel Interference Factors for High-Lift Wings in Closed Wind Tunnels*, NASA CR-2191, February 1973.)

Numerical analysis of these equations for several aspect ratios in given in Table A1.

Table A1. The norm of T for a
simple square tunnel.

AR	b/H	0.8	0.6	0.4
1		1.7586	0.8634	0.4077
2		0.7756	0.4372	0.2146
4		0.4733	0.2922	0.1416

It can be summarized that the norm of T decreases as b/H decreases
or when the aspect ratio increases.

Since convergence requires that the norm of T be less than one,
then the example illustrates that the convergence requirement will
not impose practical limitations on the use of a given wind tunnel.